Evidence of high Ca uptake by cyanobacteria forming intracellular CaCO3 and impact on their growth

Alexis de Wever, Karim Benzerara, Margot Coutaud, Géraldine Caumes, Melanie Poinsot, Fériel Skouri-panet, Thierry Laurent, Elodie Duprat, Muriel Gugger

Evidence of high Ca uptake by cyanobacteria forming intracellular $CaCO_3$ and impact on their growth

Running title: Ca homeostasis in cyanobacteria

De Wever Alexis[1], Benzerara Karim[1*], Coutaud Margot[1], Caumes Géraldine[1], Poinsot Mélanie[1], Skouri-Panet Fériel[1], Laurent Thierry[2], Duprat Elodie[1], Gugger Muriel[2]

[1]Sorbonne Université, Muséum National d'Histoire Naturelle, UMR CNRS 7590, Institut de Minéralogie, de Physique des Matériaux et de Cosmochimie, 4 place Jussieu, 75005 Paris, France

[2]Collection des Cyanobactéries, Institut Pasteur, 75724 Paris Cedex 15, France

Keywords: calcium; intracellular biomineralization; cyanobacteria; ACC

* Corresponding author

Tel.: +33(0)144277542

E-mail address: karim.benzerara@upmc.fr

Published in *Geobiology*

Abstract

Several species of cyanobacteria biomineralizing intracellular amorphous calcium carbonates (ACC) were recently discovered. However, the mechanisms involved in this biomineralization process and the determinants discriminating species forming intracellular ACC from those not forming intracellular ACC, remain unknown. Recently, it was hypothesized that the intensity of Ca uptake (i.e., how much Ca was scavenged from the extracellular solution) might be a major parameter controlling the capability of a cyanobacterium to form intracellular ACC. Here, we tested this hypothesis by systematically measuring the Ca uptake by a set of 52 cyanobacterial strains cultured in the same growth medium. The results evidenced a dichotomy among cyanobacteria regarding Ca sequestration capabilities, with all strains forming intracellular ACC incorporating significantly more calcium than strains not forming ACC. Moreover, Ca provided at a concentration of 50 µM in BG-11 was shown to be limiting for the growth of some of the strains forming intracellular ACC, suggesting an overlooked quantitative role of Ca for these strains. All cyanobacteria forming intracellular ACC contained at least one gene coding for a mechanosensitive channel which might be involved in Ca in-flux as well as at least one gene coding for a Ca^{2+}/H^{+} exchanger and membrane proteins of the UPF0016 family which might be involved in active Ca transport either from the cytosol to the extracellular solution or the cytosol towards an intracellular compartment. Overall, massive Ca sequestration may have an indirect role by allowing the formation of intracellular ACC. The latter may be beneficial to the growth of the cells as a storage of inorganic C and/or a buffer of intracellular pH. Moreover, high Ca scavenging by cyanobacteria biomineralizing intracellular ACC, a trait shared with endolithic cyanobacteria, suggests that these cyanobacteria should be considered as potentially significant geochemical reservoirs of Ca.

1. Introduction

Cyanobacteria have played an important role in mediating the formation of carbonate sedimentary deposits such as stromatolites for billions of years (Golubic & Lee, 1999; Altermann, Kazmierczak, Oren, & Wright, 2006). It has been usually suggested that this occurs through extracellular carbonatogenesis (e.g., Lee, Apel, & Walton, 2004; Riding, 2006; Kamennaya, Ajo-Franklin, Northen, & Jansson, 2012; Bundeleva et al., 2014). This process may be associated with CO_2-concentrating mechanisms, which comprises a set of diverse molecular mechanisms contributing to the concentration of inorganic carbon within cells (Riding, 2006; Jansson & Northern, 2010; Jiang, Cheng, Gao, & Qiu, 2013). More specifically, bicarbonates (HCO_3^-) are incorporated actively and transformed into CO_2 within carboxysomes for fixation by ribulose-1,5-bisphosphate carboxylase/oxygenase (Price, Maeda, Omata, & Badger, 2002). This transformation releases OH^- which are balanced by the import of H^+ so that the intracellular pH of the cells keeps regulated at a near neutral value (e.g., Belkin & Boussiba, 1991; Jiang, Cheng, Gao, & Qiu, 2013). This locally raises the extracellular pH, inducing $CaCO_3$ precipitation (Merz, 1992). Moreover, the intracellular import of H^+ is associated with an export of Ca^{2+} in some cyanobacteria, which also favors extracellular $CaCO_3$ precipitation (Waditee et al., 2004). Overall, biomineralization of $CaCO_3$ by cyanobacteria has been traditionally considered as a non-controlled and extracellular process (Riding, 2006).

However, this dogma has been recently challenged by the discovery of several cyanobacterial species forming intracellular amorphous calcium carbonates (ACC) (Couradeau et al., 2012; Benzerara et al., 2014). These cyanobacteria were found in diverse environments all around the world (Ragon, Benzerara, Moreira, Tavera, & Lopez-Garcia, 2014). This ACC formation capability is a synapomorphy at least in some cyanobacterial groups and may have appeared several hundred million years ago (Benzerara et al., 2014). Interestingly, *Gloeomargarita lithophora,* which forms intracellular ACC, is the closest modern relative of

plastid and bears information on the evolution of photosynthesis in eukaryotes by endosymbiosis of a cyanobacterium sometimes during the Proterozoic (Ponce-Toledo et al., 2017). Yet, the formation of intracellular ACC in these cyanobacteria is surprising. Indeed, considering the pH and the concentrations of HCO_3^- and Ca^{2+} in the cytoplasm of cyanobacterial cells (Badger & Andrews, 1982; Belkin & Boussiba, 1991; Barrán-Berdón, Rodea-Palomares, Leganes, & Fernandez-Pinas, 2011), precipitation is not thermodynamically possible (Cam, Georgelin, Jaber, Lambert, & Benzerara, 2015). Based on the size distribution and spatial location of intracellular Ca-carbonates in diverse strains, several nucleation sites have been suggested for these precipitates, including 1) carboxysomes for cyanobacteria showing ACC inclusions throughout their cells or 2) cytoskeletal proteins for cyanobacteria with ACC inclusions located at their septum and their poles (Li et al., 2016). Blondeau et al. (2018a) showed by using cryo-electron microscopy of vitreous sections, that intracellular ACC were systematically enclosed within an envelope which could be a protein shell or a lipid monolayer, suggesting that chemical conditions (e.g., Ca^{2+} concentration) within these vesicles might be different from those in the cytosol and more suitable to ACC precipitation.

However, differences in ability to manage Ca between cyanobacterial strains forming intracellular ACC and other strains of cyanobacteria are still unclear. Calcium is notoriously essential for all eukaryotes or prokaryotes as it fills multiple biological roles, including cellular signaling for cell structure maintenance, gene expression, cell cycle and cell differentiation processes, such as the development of heterocysts in cyanobacteria (e.g., Dominguez, 2004). In microalgae, Ca is also an essential co-factor of the oxygen-evolving complex of photosystem II (Debus, 1992). In contrast, Ca may be toxic at high cytosolic concentrations (Clapham, 2007). Overall, the current view is that the intracellular concentration of dissolved Ca^{2+} is regulated in a tight and very low concentration range (~100 nM), involving buffers usually composed of proteins with high Ca binding-affinities, which can release or trap Ca^{2+} (e.g., Gilabert, 2012;

Dominguez et al., 2015). Intracellular ACC may serve as an additional overlooked inorganic Ca-buffer. It has been demonstrated that *Gloeomargarita lithophora* C7, *Cyanothece* sp. PCC 7425 and *Thermosynechococcus elongatus* BP-1, three cyanobacteria forming ACC inclusions, strongly incorporate dissolved Ca^{2+}, whereas *Gloeocapsa* sp. PCC 73106, which does not form intracellular ACC, incorporates only limited amounts of Ca intracellularly (Cam et al., 2018). Based on these results, Cam et al. (2018) hypothesized that the ability to strongly incorporate Ca might be a specificity of cyanobacterial strains forming $CaCO_3$ inclusions and that differences in Ca homeostasis may therefore explain why some cyanobacteria form intracellular ACC while others do not. Here, we tested that hypothesis by surveying the uptake of dissolved Ca by a much larger set of cyanobacterial strains, including some forming intracellular ACC and other not forming intracellular ACC. Moreover, we searched whether cyanobacteria forming intracellular ACC need higher amounts of Ca for growth. Last, we searched in the genomes of these cyanobacteria potentially shared genes coding proteins involved in Ca transport.

2. Material & Methods

2.1. Strains and culture conditions

Fifty-two cyanobacterial strains scattered throughout the phylogenetic tree of cyanobacteria (Fig. S1) were tested for their capability to sequester Ca (Table S1). Here, we will refer to strains forming intracellular ACC as ACC+ strains and strains not forming intracellular ACC as ACC− strains. Six of the ACC+ strains were previously studied: *Synechococcus* sp. PCC 6312, *Synechococcus lividus* PCC 6716 and PCC 6717, *Cyanothece* sp. PCC 7425, *Chroococcidiopsis thermalis* PCC 7203, and *G. lithophora* C7 (Benzerara et al., 2014). These strains were isolated from very diverse environments including mesophilic alkaline lakes, hot springs at a temperature up to 53 °C and soils (Benzerara et al., 2014). Ten additional strains

phylogenetically close to these ACC+ strains were tested for their capability to form intracellular ACC: *Cyanothece* sp. PCC 8303 (isolated from a thermal resort in the Vosges, France), PCC 8955 (isolated from JB Bokassa's swimming pool in Central African Republic) and PCC 9308, *Synechococcus* sp. PCC 6603 (isolated from a freshwater pond in California) and PCC 6715 (isolated from a hot spring in Yellowstone), *Chroococcidiopsis* sp. PCC 7432 (isolated from a water spring in Pinar del Rio, Cuba), PCC 7433 (isolated from a dried pool in Cuba), PCC 7434 (isolated from a pool in a botanical garden in Havana, Cuba), PCC 7439 (isolated from a sand beach in Romania) and PCC 9819 (Table S1). Finally, 36 strains were previously shown to not form intracellular ACC (Benzerara et al., 2014). Fifty-one strains named PCC were axenic and were available from the Pasteur culture collection of cyanobacteria (PCC). *G. lithophora* was isolated from Lake Alchichica (Couradeau *et al.,* 2012) and was not axenic but co-cultured with a single alphaproteobacterium closely related to the genus *Sandarakinorhabdus* (Moreira *et al.,* 2017). All cultures were inoculated at $1/6^{th}$, starting from liquid pre-cultures in the stationary phase. They were grown to the stationary growth phase in 40 mL of liquid BG-11 (Rippka, Deruelles, Waterbury, Herdman, & Stanier, 1979), without agitation and under continuous light (8 µmol photon. m^{-2}. s^{-1}). The composition of the BG-11 medium was (in $g.L^{-1}$): $NaNO_3$: 1.5; $K_2HPO_4.3H_2O$: 0.04; $MgSO_4.7H_2O$: 0.075; $CaCl_2.2H_2O$: 0.036; citric acid: 0.006; ferric ammonium citrate: 0.006; EDTA (disodium magnesium salt): 0.001; Na_2CO_3: 0.02; trace metal mix A5+Co: 1 ml.L-1; vitamin B12: 10 pg. L-1. Trace metal mix A5+Co contained (in g.L-1): H_3BO_3: 2.86; $MnCI_2.4H_20$: 1.81; $ZnSO_4.7H_2O$: 0.222; $Na_2MoO_4.2H_2O$: 0.390; $CuSO_4.5H_2O$: 0,0.079; $Co(N0_3)_2.6H_2O$: 0.0494. Most cultures were grown at 22°C except *Cyanobacterium aponinum* PCC 10605, grown at 25°C, and the thermophilic strains such as *Synechococcus lividus* PCC 6716 and PCC 6717 as well as *Fischerella* sp. PCC 9431, which were grown at 37°C.

In parallel to the survey of Ca uptake by these 52 cyanobacterial strains, the growth of 3 planktonic ACC+ strains (*G. lithophora* C7, *Cyanothece* sp. PCC 7425 and *Synechococcus* sp. PCC 6312) and 2 planktonic ACC− strains (*Synechococcus elongatus* PCC 7942 and *Synechocystis* sp. PCC 6803) were monitored in duplicates with a higher temporal precision at two different Ca^{2+} initial concentrations: 50 µM and 250 µM. Both concentrations are environmentally relevant and typical of Ca concentrations encountered in alkaline/soda lakes such as Lake Alchichica, where *G. lithophora* was first found (e.g., Zeyen et al., 2019; Boros and Kolpakova, 2018). The standard Ca concentration in BG-11 is 250 µM. The concentration of 50 µM corresponds to the standard Ca concentration in BG-11 divided by 5 and allows to keep a concentration high enough so that it can be simply monitored over time.

Cultures were grown at 30°C, under continuous light (5 - 10 µmol photon. m^{-2}. s^{-1}) and continuous agitation (120 rpm) for all strains, except *G. lithophora* C7 which was grown under lower light intensity (2.5 - 5 µmol photon. m^{-2}. s^{-1}). In one experiment, cultures of these 5 strains grown at an initial Ca concentration of 50 µM were split in half after 22 days of cultures. Calcium was subsequently added to half of these subcultures at a concentration of 200 µM to complement the initial deficit of Ca compared to the 250 µM of Ca in standard BG-11. No Ca was added to the other half of the cultures.

2.2. Growth measurements

For comparison of Ca uptake by the fifty-two strains, growth was assessed by dry weight measurements since some of the strains tended to form aggregates and could not be simply numbered by optical density (OD) measurements. For this purpose, 200 µL of cultures were deposited on 0.22 µm GTTP filters (Millipore) weighed beforehand using an XP6 ultra microbalance (Mettler-Toledo). The GTTP filters were weighed after one week of drying at 45°C. The difference between the weight before and after filtering of the cultures provided the

mass of dry matter in $g.L^{-1}$. Measured cell masses in 200 µL of culture amounted between 18 and 848 µg depending on the strains. The precision on this measurement was 1 µg. Cell growth of the five planktonic strains cultured with 50 and 250 µM of Ca was compared by measuring optical density at 730 nm (OD_{730}) every 2 to 3 days. The instrumental precision on OD measurements was 0.005.

2.3. Chemical analyses

The concentration of dissolved Ca and the pH of the cultures were systematically measured at the stationary phase for all fifty-two strains. Solution pH was measured on 0.5 µL of non-filtered culture samples using a combined pH microelectrode (Fisherbrand). The accuracy of pH measurements was estimated at ~0.01 units. The dissolved Ca concentrations were measured by inductively coupled plasma atomic emission spectrometry (ICP-AES), using a Thermo Scientific iCAP 6200 ICP emission spectrometer. For this purpose, cultures were filtered at 0.22 µm. Depending on samples, from 200 to 400 µL of the filtrate were diluted in 10 mL of 2% HNO_3. Three measurements were performed for each sample. The 2% HNO_3 solution was analyzed as a control to assess the contamination of the HNO_3 reagent by Ca^{2+}. The Ca contamination was always lower than 6 ppb.

2.4. Transmission electron microscopy

Transmission electron microscopy analyses were performed on the ten PCC strains not tested before for their capability to form intracellular ACC. Moreover, six ACC− strains were analyzed to determine the chemical composition of their polyphosphate granules. For these analyses, 0.5 mL of the cultures were centrifuged at 5000 g for 10 min. The cell pellets were washed three times with milli-Q water and resuspended in 0.5 mL of milliQ water for analyzis by scanning transmission electron microscopy (STEM). Washing was necessary to avoid the

precipitation of salts upon drying but did not alter intracellular ACC as shown by Blondeau et al. (2018b). After washing, 3 µL of the cell suspensions were deposited on 200 mesh Formvar™ carbon coated copper grids and dried at room temperature. The grids were made hydrophilic beforehand by glow discharge, i.e. exposition for 30 s to an Ar^+ plasma. STEM analyses were performed using a JEOL 2100F microscope equipped with a field emission gun and operating at 200 kV. STEM images were acquired in the high angle annular dark field (HAADF) mode with a probe size of 0.7 to 1 nm. Elemental mapping was performed based on energy dispersive x-ray spectrometry (EDXS) analyses using the JEOL Analysis Station software. Semi-quantitative analyses of EDXS spectra were processed to assess the Ca/Mg ratios of the polyphosphate in the cells following the procedure by Li et al. (2016) based on the use of K factors which provide the relationship between peak intensity and the element quantity. The hypothesis that Ca/Mg ratios of the polyphosphate granules were significantly different between ten ACC+ strains (number of polyphosphate granules, n=136) and six ACC− strains (n=133) was tested by a statistical non-parametric Wilcoxon-Mann-Whitney procedure, which does not require the assumption of normal distributions. This analysis was performed using the software R version 3.2.0 (Team, 2013).

2.5. Search of Ca-related transport genes in the genomes of cyanobacteria forming intracellular ACC

Several families of Ca-related transport proteins have been described in the literature. Three hundred and thirty-nine reference sequences of known proteins involved in Ca transport were retrieved from the transporter classification database (TCDB, Saier et al., 2015) by using the substrate search tool (with Ca as requested substrate). Their homologs were searched in all the available genomes of cyanobacteria forming intracellular ACC (Table 1) by BLAST with an e-value threshold of 1e-05, resulting in 4280 sequences. Each sequence was further searched for

similarity with known domain profiles using CD-search (Marchler-Bauer et al., 2016; CDD database, version 3.6). The best specific hit (according to the hit classification provided by CD-search) was kept to validate the functional annotation of the sequences and their specific implication in Ca transport. As the genomes of PCC 6716 and PCC 6717 have not been structurally annotated yet, their genomic sequences were explored using tBLASTn in order to search for homologs of the Ca-related proteins previously found in the five other genomes. The hits were further validated with CD-search. Transport proteins shared by ACC+ strains were also searched in the available genomes of ACC- strains.

Transport type	Function	specific hit (CDD profile)	*G. lithophora C7*	*S.* sp. PCC 6312	*S. lividus* PCC 6715	*S. lividus* PCC 6716	*S. lividus* PCC 6717	*C. thermalis* PCC 7203	*C.* sp. PCC 7425	Reference
			NZ_CP017675.1	NC_019680.1	NZ_CP018092.1	Unpublished		NC_019695.1	NC_011884.1	
Active transport	Ca^{2+}ATPase	cd02089	0	0	0	0	0	AFY89136.1, AFY89473.1	ACL44608.1	Berkelman, Garret-Engele, & Hoffman, 1994
	apnhaP (K^+/H^+ antiporter, Ca^{2+}/H^+ antiporter at alkaline pH)	COG0025	APB33279.1	AFY60943.1, AFY61477.1, AFY62329.1	ATS18144.1	1	1	AFY86316.1, AFY86773.1, AFY88512.1, AFY89267.1, AFY89685.1	ACL43274.1, ACL45641.1, ACL45953.1, ACL47119.1	Waditee et al., 2001
	UPF0016 (Putative Ca^{2+}/cation antiporter)	COG2119, pfam01169	APB33251.1, APB33252.1	AFY59528.1, AFY61632.1, AFY62270.1	ATS18363.1, ATS18364.1	1	1	AFY86178.1, AFY86627.1, AFY86628.1	ACL43789.1, ACL46990.1, ACL46991.1	Demaegd et al., 2014
	Ca^{2+}/H^+ antiporter	COG0387	APB32733.1	AFY62574.1	ATS17843.1	1	1	AFY88666.1, AFY88667.1	ACL43313.1, ACL45336.1	Domínguez, Guragain, & Patrauchan, 2015
	Ca^{2+}/Na^+ antiporter	pfam01699	APB34699.1	0	ATS18027.1	0	1	AFY89133.1	ACL44147.1, ACL45335.1	
Passive transport	Mechanosensitive channel	COG0668	APB35048.1	AFY61749.1	0	0	0	AFY88096.1, AFY88215.1, AFY89282.1, AFY89283.1	0	
		pfam00924	APB33494.1, APB33956.1, APB32821.1, APB32856.1	AFY60788.1, AFY59468.1, AFY62613.1	ATS17940.1, ATS18073.1	3	2	AFY88498.1	ACL43383.1, ACL43916.1, ACL44170.1, ACL46737.1, ACL47385.1	
	hBI-1(pH sensitive channel)	pfam01027	0	AFY61003.1	ATS17502.1	1	1	AFY90919.1	ACL43777.1	Chang *et al.*, 2014
	Pit ($CaHPO_4/H^+$ symport)	pfam01384, COG0306	0	0	ATS18407.1	1	1	AFY87346.1	ACL43457.1	Domínguez, Guragain, & Patrauchan, 2015

Table 1. Proteins involved in Ca^{2+} transport detected in seven cyanobacterial strains forming intracellular ACC. Protein sequence identifiers (Genbank accessions) are reported.

2.6. Phylogenetic analyses

The 16S rRNA gene sequences were retrieved from genomes and aligned using CLUSTAL_W (Thompson, Higgins, & Gibson, 1997). One thousand four hundred and fifteen conserved positions in the sequences were considered in order to compute a phylogenetic tree using PHYML (Guindon et al., 2003) and applying the Gamma Time Reversible model. One hundred bootstrap replicates were performed to assess the statistical support of each node and the ones with a value greater than 70% were kept. The sequences were retrieved from GenBank under the accession numbers MK484706 to MK484714.

3. Results

3.1. Assessing the capability of cyanobacterial strains to form intracellular ACC

Among the fifty-two cyanobacterial strains studied here, six strains (*Synechococcus* sp. PCC 6312, PCC 6716 and PCC 6717, *Cyanothece* sp. PCC 7425, *Chroococcidiopsis* sp. PCC 7203, and *G. lithophora* C7) were already known to form intracellular ACC (Benzerara *et al.,* 2014). Additionally, ten strains phylogenetically close to some of these ACC+ strains were tested for their capability to form intracellular ACC (Table S1) : *Cyanothece* sp. PCC 8303, PCC 8905 and PCC 9308 were close relatives of *Cyanothece* sp. PCC 7425; *Synechococcus lividus* PCC 6715 and *Synechococcus* sp. PCC 6603 were close relatives of *S. lividus* PCC 6716 and PCC 6717 and *Synechococcus* sp. PCC 6312, respectively; *Chroococcidiopsis* sp. PCC 7432, PCC 7433, PCC 7434, PCC 7439 and PCC 9819 were close relatives of *Chroococcidiopsis thermalis* PCC 7203 (Fig. S1). STEM-EDXS analyses showed that these ten strains were also capable to form intracellular ACC in BG-11 (Fig. 1). Cells of *Synechococcus* sp. PCC 6715 and PCC 6603 showed ACC inclusions mostly located at their poles as in *Synechococcus* sp. PCC 6312 and *S.*

lividus PCC 6716 and 6717. In contrast, the cells of all other ACC+ strains showed inclusions scattered throughout the cells similarly to *Cyanothece thermalis* PCC 7425 and *Chroococcidiopsis* sp. PCC 7203. Overall, among the 52 analyzed strains, 16 strains formed intracellular ACC, while 36 did not form intracellular ACC.

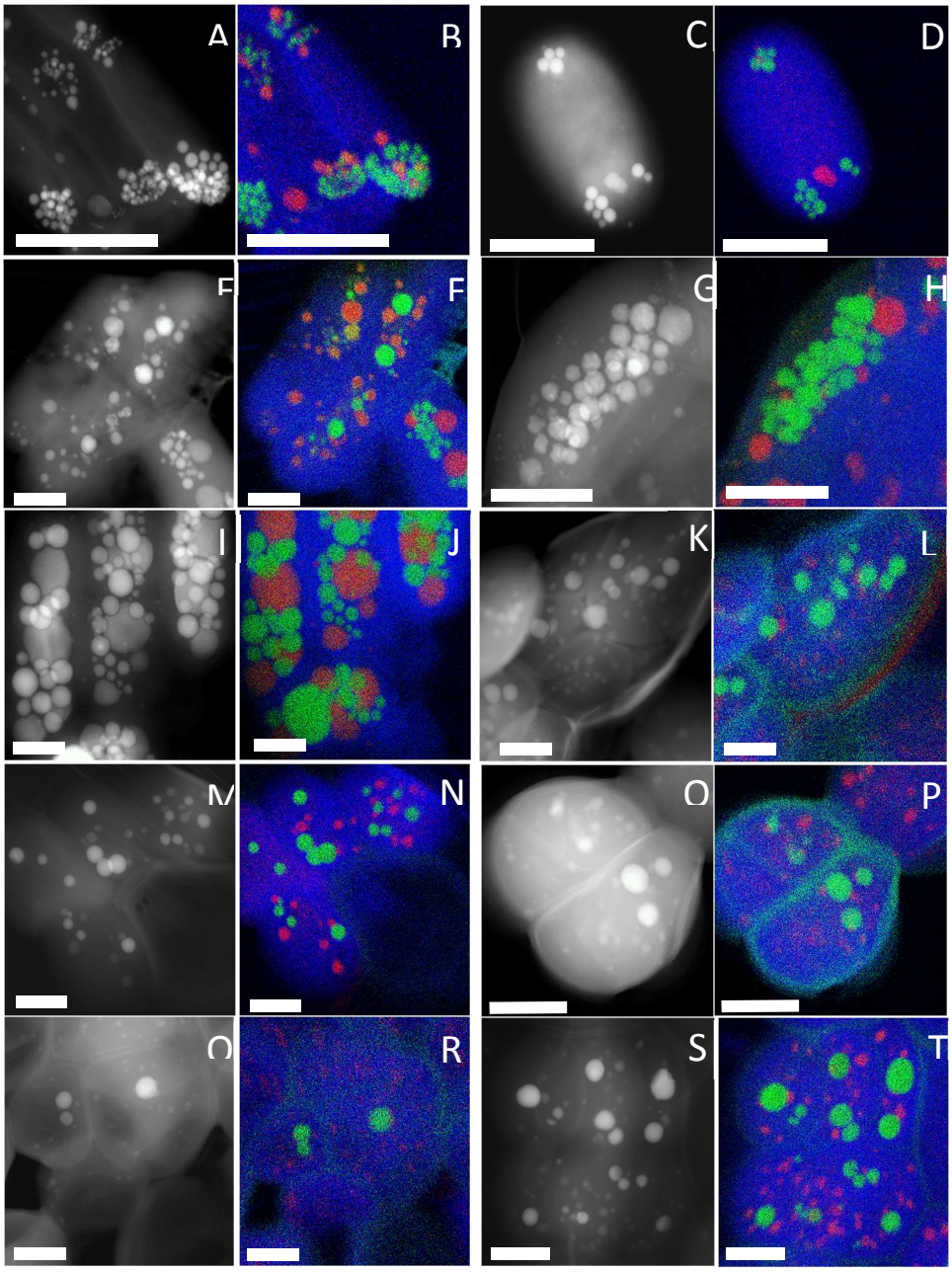

Figure 1. STEM HAADF-EDXS analyses of the 10 strains tested for their capability to form intracellular ACC. (A) and (B): STEM-HAADF image and EDXS map of *Synechococcus* sp. PCC 6715. (C) and (D): *Synechococcus* sp. PCC 6603. (E) and (F): *Cyanothece* sp. PCC 8303. (G) and (H) *Cyanothece* sp. PCC 8955. (I) and (J) *Cyanothece* sp. PCC 9308. (K) and (L) *Chroococcidiopsis* sp. PCC 7432. (M) and (N) *Chroococcidiopsis* sp. PCC

7433. (O) and (P) *Chroococcidiopsis* sp. PCC 7434. (Q) and (R) *Chroococcidiopsis* sp. PCC 7439. (S) and (T) *Chroococcidiopsis* sp. PCC 9819. For all EDXS maps, calcium is in green, phosphorus in red and carbon in blue. As a result, Ca-carbonates appear in green and PolyP granules in red. All scale bars represent 2 µm.

As evidenced by EDXS maps, Ca was mostly contained in intracellular ACC inclusions for these ten strains similarly to their ACC+ relatives. Some Ca was also detected by STEM-EDXS in association with the polyphosphate granules in these strains, which mostly contained Mg as a counter-cation (Fig. 2 and Fig. S2). Interestingly, some Ca was also detected in the polyphosphate inclusions of some of the six strains not forming intracellular $CaCO_3$ that were analyzed in this study (*Gloeocapsa* sp. PCC 7428, *Synechocystis* sp. PCC 6803, *Oscillatoria* sp. PCC 6304, *Cyanobium gracile* PCC 6307, *Synechococcus* sp. PCC 6301, *Leptolyngbya* sp. PCC 7104). Based on a Wilcoxon-Mann-Whitney statistical analysis, the Ca/Mg ratio of polyphosphates was shown to be significantly higher in ACC+ strains than in ACC− strains (Fig. 2). In one ACC− strain, *Gloeocapsa* sp. PCC 7428, STEM observations showed that a significant amount of Ca was localized on/in the cell wall of the cells, in association with K, Mg and S (Fig. S3).

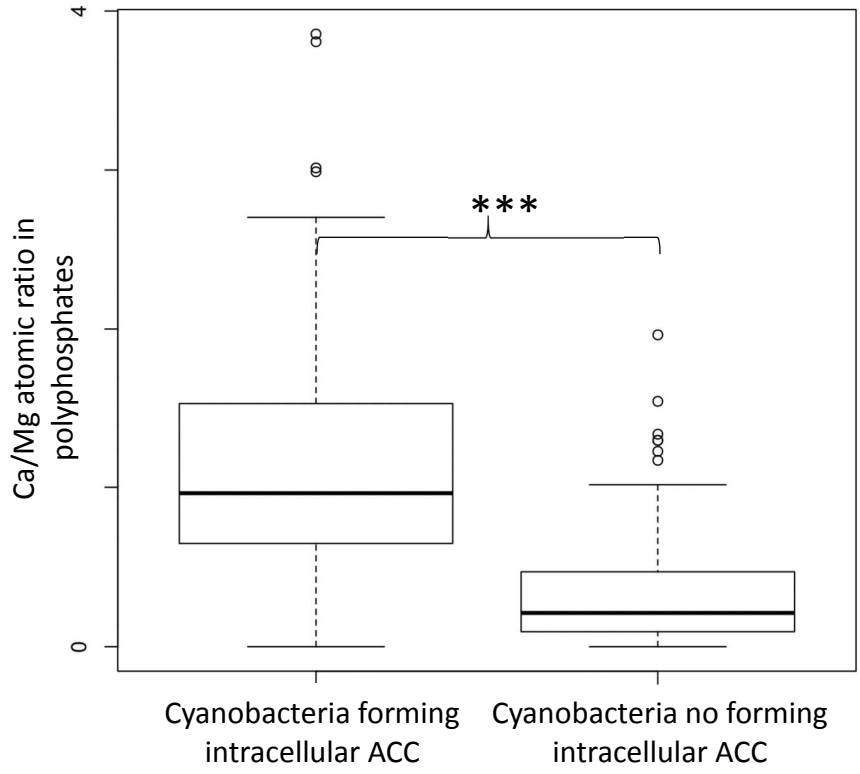

Figure 2. Ca/Mg atomic ratio of polyphosphates in strains forming intracellular ACC (left) vs. strains not forming intracellular ACC (right). The dataset includes the Ca/Mg ratios of 136 polyphosphates from ten strains forming intracellular ACC and 133 polyphosphates from six strains not forming intracellular ACC. The Ca/Mg values of the polyphosphates were calculated based on STEM-EDX analyses. The bold lines indicate the median values; the boxes span the second and third quartiles; the vertical dashed lines span 1.5 times the extent of the boxes. Open circles are outliers. The Wilcoxon-Mann-Whitney statistical analysis shows that the difference between the two groups is significant *** $p < 0.001$.

3.2. Assessment of the Ca uptake by the 52 cyanobacterial strains

The 52 cyanobacterial strains analyzed in this study were cultured in the same BG-11 medium (Table S1). The initial concentration of dissolved Ca^{2+} was measured at 281 µM (±6). The final concentration of dissolved Ca^{2+} was measured after 40 to 61 days of incubation depending on the strains. This final concentration widely varied between strains (Fig. 3). Many strains (36 out of 52) showed little to no Ca uptake, i.e. less than 22% of the initial Ca stock available in the solution. *Gloeocapsa* sp. PCC 7428 showed an intermediate uptake of ~38% of the initial

300 Ca^{2+} concentration. Sixteen strains showed a high Ca uptake, i.e. higher than 58% of the initial
301 Ca stock and up to ~98% for *G. lithophora* C7. The very high Ca uptake correlated with the
302 capability of the strain to form intracellular ACC: all 16 ACC+ strains showed a Ca uptake
303 higher than ACC− strains (Fig. 3). Significance of this difference was supported by a Wilcoxon-
304 Mann-Whitney statistical analysis with p <0.001.

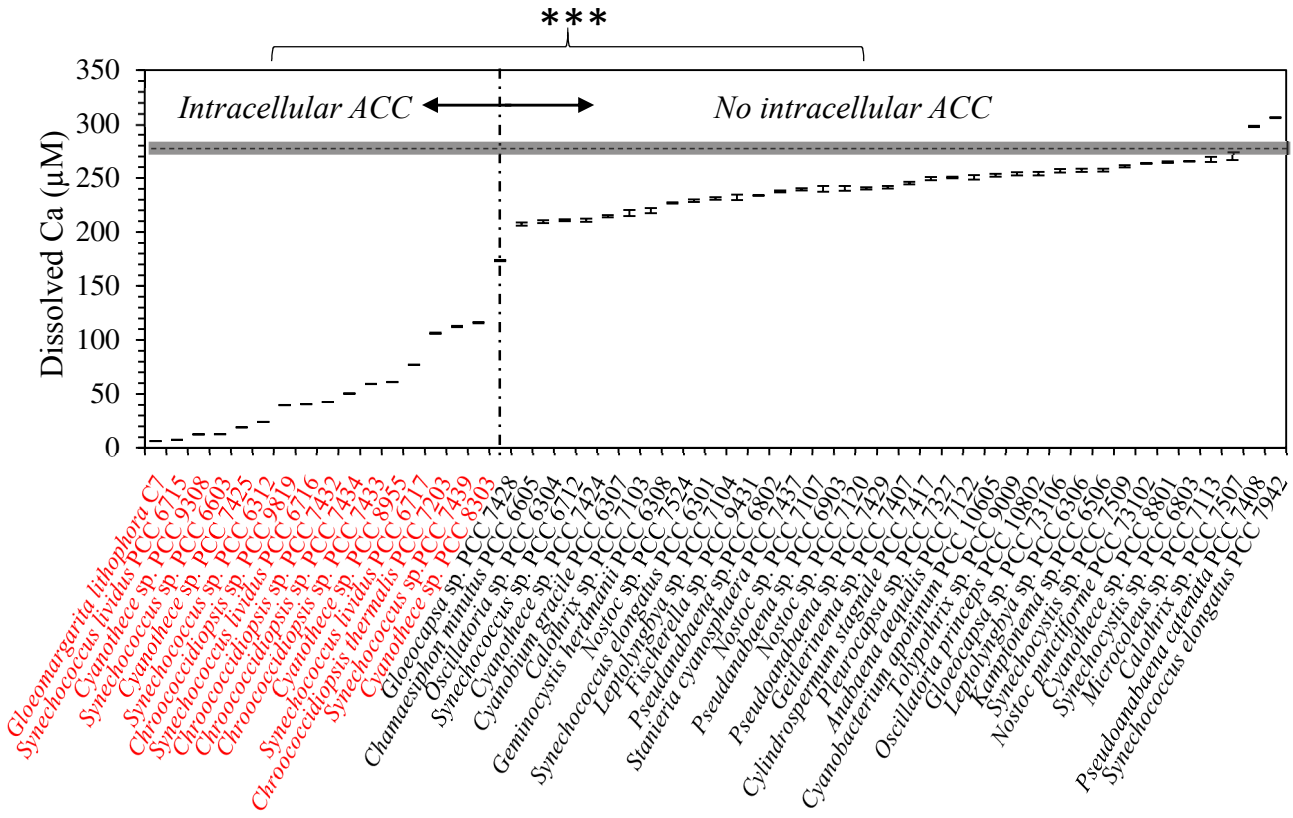

305

306 **Figure 3.** Plot of the concentrations of dissolved calcium remaining after 40 - 61 days of incubation for the 52
307 tested strains. In red: strains forming intracellular calcium carbonates; in black: strains not forming intracellular
308 carbonates. The dashed line represents the initial concentration of dissolved calcium in the culture medium (BG-
309 11). The grey area corresponds to error bars around this value. Error bars were calculated based on the precision
310 of ICP-AES.

311

312 Since parameters other than the capability of the cells to form intracellular ACC such as pH,
313 the final dry mass and incubation duration may *a priori* impact the observed variability of Ca

uptake, we tested potential correlations between Ca uptake and these parameters. While the initial pH of the BG-11 medium was 7.5, it systematically increased upon cell growth, reaching a final value between 8 and 11 depending on the strains. No correlation was detected between the final pH and Ca uptake (Fig. S4). Similarly, different strains showed different final dry masses, but dry masses were not correlated with Ca uptake (Fig. S5). Last, we tested the influence of an incubation time of 40 *vs* 60 days on Ca uptake for three ACC+ strains and two ACC- strains (Fig. S6). Although we observed that uptake increased from 53% to 92% between 40 and 60 days for *Synechococcus* sp. PCC 6312, the ranking of the strains in terms of Ca uptake did not vary over this time range. This is also consistent with the analyses by Cam et al (2018), who showed that Ca uptake rate was higher in the first hours of cultures of several ACC+ strains. Overall, these tests supported the conclusion that cultures of ACC+ strains intrinsically showed a higher Ca uptake than ACC− strains regardless of their dry masses, the duration of incubation (40 or 60 days) and/or extracellular pH.

3.3. Impact of the initial concentration of dissolved Ca^{2+} on the growth of cyanobacteria forming intracellular ACC

We selected a subset of three strains representing the two types of intracellular ACC distributions: scattered through the cell, i.e. *G. lithophora* C7 and *Cyanothece* sp. PCC 7425, and at the cell poles: *Synechococcus* sp. PCC 6312. Their growth was compared with that of two ACC− strains: *Synechococcus elongatus* PCC 7942 and *Synechocystis* sp. PCC 6803. The growth of these three ACC+ strains and two ACC− strains was measured in BG-11 at two initial Ca^{2+} concentrations: 50 µM and 250 µM. *G. lithophora* C7 and *Cyanothece* sp. PCC 7425 showed significantly higher growth rates when grown with an initial Ca concentration of 250 µM compared to 50 µM (Fig. 4). In contrast, growth was only slightly higher for *Synechococcus* sp. PCC 6312 at an initial Ca concentration of 250 µM (compared to 50 µM) and not significantly different between the two Ca concentrations for *Synechocystis* sp. PCC 6803 and

S. elongatus PCC 7942. The pH showed similar differences between cultures at 50 and 250 µM, reaching significantly higher values at 250 µM for *G. lithophora* C7 and *Cyanothece* sp. PCC 7425 but similar values at 50 and 250 µM for *Synechococcus* sp. PCC 6312, *S. elongatus* PCC 7942 and *Synechocystis* sp. PCC 6803 (Fig. S7).

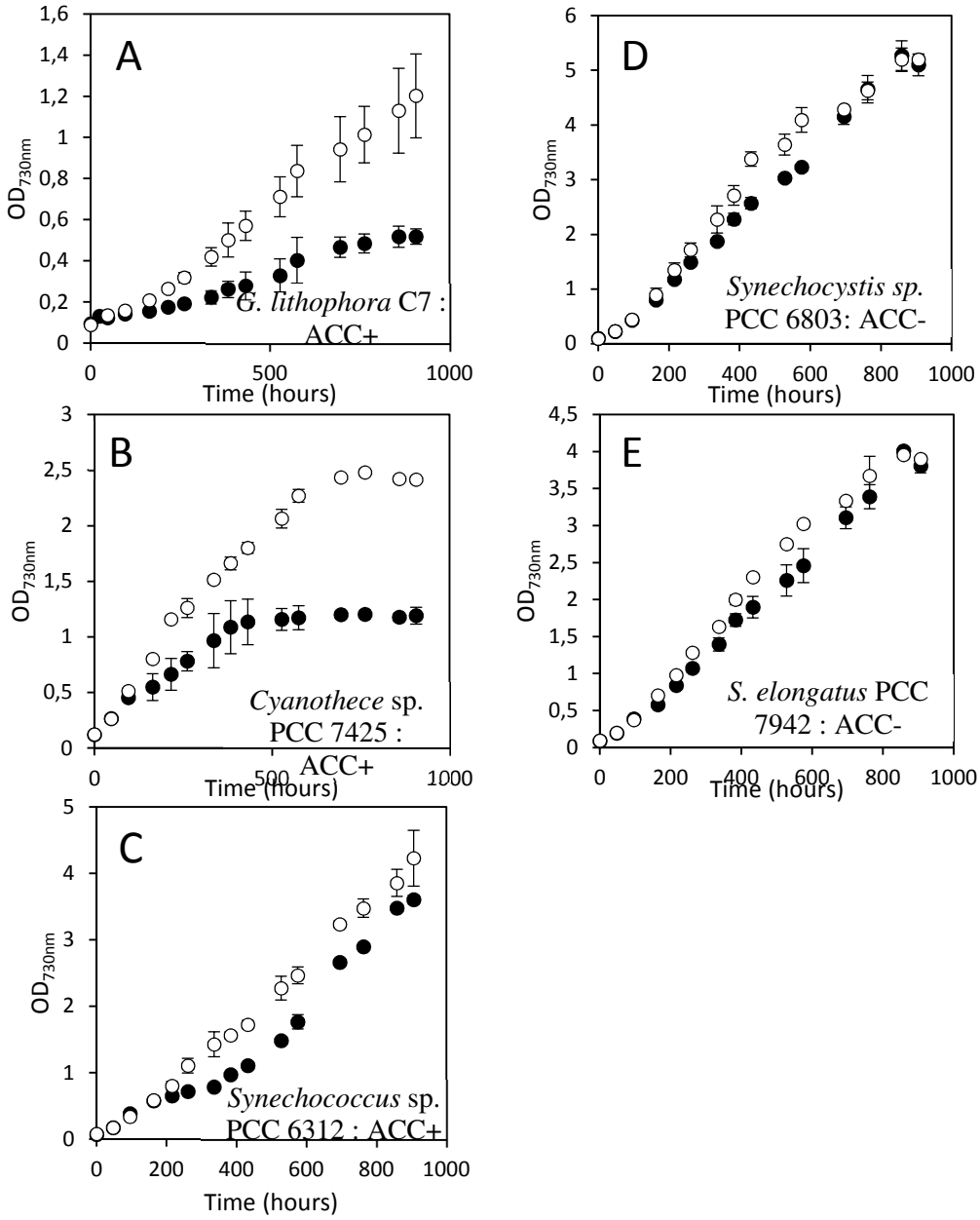

Figure 4. Time evolution of OD_{730nm} for cultures in a BG-11 medium with an initial dissolved Ca concentration of 250 µM (open symbols) and 50 µM (closed symbols). (A) *G. lithophora* C7; (B) *Cyanothece* sp. PCC 7425; (C) *Synechococcus* sp. PCC 6312; (D) *Synechocystis* sp. PCC 6803; (E) and

S. elongatus PCC 7942. Error bars represent standard deviations calculated based on variations between duplicates.

To further test the growth dependence on the Ca content of the growth medium, cultures with 50 μM of Ca were split in half after 527 hours. Calcium was subsequently added to half of these subcultures at a concentration of 200 μM to complement the initial deficit of Ca compared to the 250 μM of Ca in standard BG-11. No Ca was added to the other half of the cultures. For *G. lithophora*, the culture was still growing at the time of Ca addition (Fig. 5). Yet, 300 h after Ca addition, the Ca-supplemented subcultures reached an OD_{730} significantly higher than the subcultures with no Ca addition. The difference was even larger for *Cyanothece* sp. PCC 7425. These differences could also be observed on the time evolution of pH (Fig. S8). In contrast, the OD_{730} of the Ca-supplemented subculture of *Synechococcus* sp. PCC 6312 was slightly lower than that with no Ca addition (Fig. 5). The time evolution of the pH was similar for the two subcultures (Fig. S8). For Synechocystis sp. PCC 6803 and S. elongatus PCC 7942, subcultures with no Ca addition reached significantly higher OD_{730} than Ca-supplemented subcultures (Fig. 5).

3.4. Genome analyses

Genes coding for proteins possibly involved in passive and active transport of Ca were searched and quantified in the annotated genomes of seven ACC+ strains (Table 1). Regarding active transport, all genomes contained at least one copy (e.g., two for *Cyanothece* sp. PCC 7425 and *Chroococcidiopsis thermalis* PCC 7203) of a gene coding for a Ca^{2+}/H^{+} exchanger and between one and three copies of the UPF0016 gene coding for a putative calcium/cation exchanger (Demaegd, Colinet, Deschamps, & Morsomme, 2014). All these genomes also encoded a homolog of a Na^{+}/H^{+} antiporter (apnhaP) that has been reported to have a high Ca^{2+}/H^{+} antiport activity at alkaline pH (Waditee et al, 2001). In contrast, homologs of other genes coding for

371 transporters possibly involved in Ca transport (Ca^{2+} ATPase, Pit, Ca^{2+}/Na^{+} antiporter) were
372 found in some but not all these 7 genomes. Regarding passive transport, at least one copy of a
373 gene coding for a mechanosensitive channel was found in all genomes. A homolog of a pH-
374 sensitive Ca leak channel (Human Bax1 inhibitor) found in some intracellular membranes
375 (Chang et al., 2014) was detected in all genomes but the one of *G. lithophora*.

376 ## 4. Discussion

377 ### *4.1. Cyanobacteria forming intracellular $CaCO_3$ show a very strong Ca uptake*

378 Several previous studies have assessed cell Ca uptake by measuring the temporal
379 changes of dissolved extracellular Ca^{2+} concentration (Singh & Mishra, 2014; Cam et al., 2016;
380 Blondeau et al., 2018b). Yet, changes in dissolved Ca concentrations can *a priori* be due to i)
381 extracellular precipitation of Ca-containing mineral phases, ii) adsorption at the cell surfaces
382 and/or by surface EPS and/or iii) Ca uptake within cells. Here, Ca uptake within cells is argued
383 to be the most important process responsible for the observed differences in the decrease of
384 extracellular dissolved Ca concentration between cultures of ACC+ and ACC− cyanobacterial
385 strains. This conclusion relies on several lines of evidence. First, cultures with higher solution
386 pH should experience higher rates of extracellular Ca-mineral precipitation and/or cell surface
387 adsorption (Bundeleva et al., 2014; Lee, Apel, & Walton, 2004). However, no correlation was
388 detected between pH and the decrease of dissolved Ca concentrations, i.e. the pH in the culture
389 media of ACC+ strains increased to diverse values with no systematic differences with ACC−
390 strains. In some cultures, where pH increased to high values (e.g., pH = 10.56 for
391 *Synechococcus* sp. PCC 6301), only a slight decrease of dissolved Ca concentration was
392 observed ($\Delta([Ca^{2+}]) = 49.56\ \mu M$). Moreover, STEM observations clearly showed that Ca was
393 mostly contained within intracellular ACC inclusions in ACC+ strains and to a lesser extent
394 within polyphosphates. Overall, this supports the conclusion that the variations observed in the

decrease of dissolved Ca concentration was primarily dependent on the capability of the strains to form intracellular ACC. Consistently, Cam et al. (2018) showed that BG-11 remained mostly undersaturated with Ca-carbonate phases in the cultures of three ACC+ strains and that the decrease of dissolved Ca concentrations in these cultures was primarily due to Ca uptake within cells. Overall, the present study, based on the comparison between 52 strains, generalizes the hypothesis formulated by Cam et al. (2018) based on only 4 strains, that cyanobacteria forming intracellular ACC show a Ca uptake systematically higher than other cyanobacteria.

Although it is difficult to definitely demonstrate that ACC- strains never form ACC (since this would require to culture them under an infinite number of diverse conditions), it can be concluded that they do not form ACC at least under the specific conditions used here in the present study. Moreover, it should be noted that some of them (e.g., PCC 6803, PCC7942) have been scrutinized at different time points, therefore providing a much more extensive sampling of diverse conditions. Last, we note that under the specific culture conditions we used, there is a relationship between forming/not forming iACC and phylogeny (Fig. S1). This suggests that this trait may be a synapomorphy for the *Chroococcidiopsis* and the *Cyanothece* sp PCC 7425 clusters as already mentioned for the *Synechococcus* sp. PCC 6312 cluster by Benzerara et al. (2014) and that it is likely more controlled by genetics than environmental conditions.

4.2. Relatively high Ca adsorption by Gloeocapsa sp. PCC 7428

Although *Gloeocapsa* sp. PCC 7428 showed an affinity for Ca lower than ACC+ cyanobacteria, it was significantly higher than other ACC− cyanobacteria. STEM analyses showed that Ca was clearly associated with the cell walls of *Gloeocapsa* sp. PCC 7428. Cell walls of *Gloeocapsa* sp. PCC 7428 have been shown to be composed of a thick extracellular sheath of mucopolysaccharides (Gonzalez-Esquer *et al.,* 2016), which may therefore be responsible for this relatively high Ca sorption capability. Whether this is due to a high surface

Ca adsorption capacity of the strain and/or precipitation of extracellular Ca-mineral phases could not be determined here but it is known that there is a continuum between surface adsorption and extracellular mineral precipitation (Warren & Ferris, 1998). Consistently, several studies have stressed on the significant calcification potential of the genus *Gloeocapsa* (Pokrovsky, Martinez, Golubev, Kompantseva, & Shirokova, 2008; Bundeleva et al., 2014). Moreover, cyanobacteria of the Chroococcales order, to which *Gloeocapsa* sp. PCC 7428 belong, have been proposed more generally to be particularly efficient at precipitating Ca-carbonates (e.g., Saghai et al., 2015). Overall, the present survey of a large number of cyanobacterial strains supports the idea that *Gloeocapsa* sp. PCC 7428 may be particularly prone among cyanobacteria at inducing the precipitation of extracellular Ca-mineral phases.

4.3. Comparison of the Ca content of ACC+ cyanobacterial strains with other known bacteria

Here, we normalized the Ca uptake by ACC+ strains to their dry weight and compared them with similar data found in the literature for other bacteria (Table 2). As discussed by Cam et al. (2018), these values did not represent the maximum values that may be achieved by these strains as Ca input was limited to 250 µM in these batch cultures. Yet, the cell-normalized Ca contents measured on cyanobacteria forming intracellular ACC are among the highest content reported in the literature. As a comparison, more classically studied bacteria such as *Escherichia coli*, *Vibrio cholera* or *Acetobacter aceti* contain two orders of magnitude less Ca. In contrast, there are few other bacteria accumulating Ca to a high extent. For example, *Achromatium* spp., a gammaproteobacterium forming intracellular calcite is to our knowledge the strongest Ca-accumulating bacterium that has been reported so far, with a Ca content of 65400 fmol of Ca per cell (Gray, 2006). Assuming that the mass of C represents 50% of dry weight, a carbon-to-volume conversion of 0.1 pgC/µm^3 for bacteria (Norland, Heldal, & Tumyr,

444 1987) and a cell volume of $3x10^4$ μm^3 (Gray, 2006), this equals to 436 mg of Ca per gram of
445 dry matter, i.e. an order of magnitude higher than for cyanobacteria forming intracellular ACC.
446 *Bacillus cereus* spores also sequester high amounts of Ca on the same order of magnitude as
447 cyanobacteria forming intracellular ACC but with a different speciation, i.e. as Ca^{2+}-dipicolinic
448 acid chelates, incorporated in the spore cores (Steward, 1980).

Name	Type of organism	Ca uptake		Notes	Reference
		[HC1]mg/g of dry matter	fmol/cell		
	Archaea				
Haloferax volcanii		0.36			Novoselov et al., 2017
Natrialba magadii		0.31			Novoselov et al., 2017
	Bacteria				
	Actinobacteria				
Micrococcus roseus		0.08			Rouf, 1964
Nesterenkonia lacusekhoensis		0.06			Novoselov et al., 2017
	Firmicute				
Alicyclobacillus acidoterrestris		0.39			Novoselov et al., 2017
Bacillus cereus (vegetative cells)		0.3			Rouf, 1964
Bacillus cereus (spores)		28.00 to 30.00			Steward et al., 1980
	Proteobacteria				
Acetobacter aceti		0.07			Novoselov et al., 2017
***Achromatium* spp.**		436	65400	intracellular calcite	Gray, 2006
Alcaligenes marinus		0.09			Jones, Royle, & Murray, 1979
Escherichia coli		3.21			Novoselov et al., 2017
		1.10			Lawford & Rousseau, 1995 ; Demain & Solomon 1981
		0.11			Novoselov et al., 2017
		0.11			Novoselov et al., 2017
		0.07			Novoselov et al., 2017
		0.06			Novoselov et al., 2017
		0.06			BioMagnetech Corporation, 1990
		0.02			Rouf, 1964
Sphaerotilus natans		0.18			Rouf, 1964
Vibrio cholerae		0.09			Novoselov et al., 2017
	Cyanobacteria				
***Chroococcidiopsis* sp. PCC 7432**		8.88		intracellular ACC	This study
***Chroococcidiopsis* sp. PCC 7433**		11.09		intracellular ACC	This study
***Chroococcidiopsis* sp. PCC 7434**		12.55		intracellular ACC	This study
***Chroococcidiopsis* sp. PCC 7439**		11.09		intracellular ACC	This study
***Chroococcidiopsis* sp. PCC 9819**		8.36		intracellular ACC	This study
***Chroococcidiopsis thermalis* PCC 7203**		6.58		intracellular ACC	This study
***Cyanothece* sp. PCC 7425**		17.92	5.4	intracellular ACC	This study
		13.00	3.9	intracellular ACC	Cam et al., 2018
***Cyanothece* sp. PCC 8303**		17.13		intracellular ACC	This study
***Cyanothece* sp. PCC 8955**		22.57		intracellular ACC	This study
***Cyanothece* sp. PCC 9308**		37.69		intracellular ACC	This study
***Gloeocapsa* sp. PCC 7428**		8.34		adsorption/ precipitation	This study
***Gloeomargarita lithophora* C7**		31.41	2.7	intracellular ACC	This study
		26.00	1.7	intracellular ACC	Cam et al., 2018
Mastigocoleus testarum		20.00	100	calcicyte	Guida & Garcia-Pichel, 2016
***Microcystis aeruginosa* Kützing**		0.44			Krivtsov, Bellinger, & Sigee, 2005
***Synechococcus* sp. PCC 6312**		29.13		intracellular ACC	This study
***Synechococcus* sp. PCC 6603**		42.82		intracellular ACC	This study
***Synechococcus lividus* sp. PCC 6715**		25.46		intracellular ACC	This study
***Synechococcus lividus* sp. PCC 6716**		15.15		intracellular ACC	This study
***Synechococcus lividus* sp. PCC 6717**		33.99		intracellular ACC	This study
***Thermosynechococcus elongatus* BP-1**		15.00	4.8	intracellular ACC	Cam et al., 2018

450 **Table 2**. Ca uptake by diverse prokaryotes compiled from the literature and our data.

451 Among cyanobacteria, the differentiated cells called calcicytes, observed in the
452 filamentous euendolithic cyanobacterium *Mastigocoleus testarum* have been measured to
453 contain 100 fmol of Ca per cell, which measured ~$1x10^3$ μm^3 (Guida & Garcia-Pichel, 2016).
454 This represents 20 mg of Ca per g of dry weight, a value similar to that estimated for
455 cyanobacteria forming intracellular ACC (**Table 2**). The speciation of Ca in calcicytes has not
456 been determined so far and the possibility that it is mostly contained in intracellular ACC has
457 not been yet explored to our knowledge. Moreover, Cam et al. (2018) noted that since some
458 cyanobacteria forming intracellular ACC tend to decrease the extracellular concentration of
459 dissolved Ca^{2+}, they may favor the dissolution of extracellular Ca-carbonates. This conclusion
460 can be generalized to all cyanobacteria forming intracellular ACC and future studies should
461 investigate their capabilities to bore into calcium carbonate crystals.

462 *4.4. Molecular mechanisms of high Ca sequestration*

463

464 Whether cyanobacteria forming intracellular ACC may share Ca-sequestering
465 molecular pathways that are similar and possibly homologous to those of *Mastigocoleus*
466 *testarum,* would be interesting to test in future studies. Since Ca uptake involves Ca transport
467 proteins in any case, we searched genes that might be shared by the seven genomes available
468 for the divergent strains forming intracellular ACC.

469 The influx (from the extracellular solution to the cytosol) of Ca is usually assumed to
470 occur passively through channels, which show little ionic specificity for most of them
471 (Domínguez, Guragain, & Patrauchan, 2015). Here, a mechanosensitive channel was shown to
472 be present in all the ACC+ cyanobacteria. However, it should be noted that mechanosensitive
473 channels can also be found in ACC- cyanobacteria, such as *Synechocystis* sp. PCC 6803
474 (Nazarenko, Andreev, Lyukevich, Pisareva, & Los, 2003). Interestingly, inorganic phosphate

475 transport systems (PitB in *E. coli*) also seem able to transfer divalent cation-HPO_4 neutral
476 complexes intracellularly under some conditions (van Veen, Abee, Kortstee, Konings, &
477 Zehnder, 1994). This could connect Ca uptake with P sequestration which results in the
478 formation of polyphosphate granules in some of these cyanobacteria (e.g., Cam et al., 2018;
479 Blondeau et al., 2018a). However, these transport systems were detected in only some of the
480 ACC+ cyanobacteria.

481 The out-flux of Ca is usually assumed to occur actively through transporters. Out-flux
482 may proceed from the cytosol towards the extracellular solution or from the cytosol towards an
483 intracellular compartment as the one delimitating intracellular ACC (Blondeau et al., 2018a).
484 Here, we identified in all ACC+ cyanobacteria at least one gene coding for a Ca^{2+}/H^+
485 transporter, and at least one gene coding for a putative calcium exchanger of the UPF0016
486 family. Again, it should be noted that Ca^{2+}/H^+ antiports and membrane proteins of the UPF0016
487 family have been identified in numerous other bacteria (Domínguez, Guragain, & Patrauchan,
488 2015). Identifying their localization, in the plasma membrane or in intracellular compartments
489 would help deciphering if they are involved in Ca export extracellularly or within an
490 intracellular compartment. Mansor, Hamilton, Fantle, and Macalady (2015) identified in
491 *Achromatium* a Ca^{2+}-ATPase and noted that they could also be found in *C. thermalis* PCC 7203,
492 *Cyanothece* sp. PCC 7425 and *Thermosynechoccus elongatus* BP-1. Here, we confirm that a
493 Ca^{2+}-ATPase is indeed present in the genomes of *C. thermalis* and *Cyanothece* sp. but it is
494 absent from the genomes of the five other ACC+ strains. Garcia-Pichel, Ramírez-Reinat, and
495 Gao (2010) also detected a Ca^{2+}-ATPase in *Mastigocoleus testarum*, an endolithic
496 cyanobacterium but stressed that this pump extrudes Ca^{2+} outside of the cell, confirming that it
497 is not likely involved in Ca sequestration within cells.

498 Overall, this analysis provides some indications about possible actors involved in Ca
499 homeostasis but it should be noted that this clearly does not provide definitive clues about the

mechanisms involved in ACC formation since: 1) similar genes might be found in ACC-cyanobacteria; 2) the diverse cyanobacteria forming intracellular ACC may use different biomineralization mechanisms involving different sets of genes; 3) formation of intracellular ACC likely involves other processes than in- and out-fluxes of Ca. Only future genetic studies targeting and deleting such candidate genes will provide definitive answers about their possible role in the future.

4.5. Cause for a high Ca demand by cyanobacteria forming intracellular ACC

Calcium at a concentration of 50 µM in BG-11 was shown to be limiting for the growth of *Cyanothece* sp. PCC 7425 and *G. lithophora* C7. In contrast, Ca was not limiting at this concentration for the growth of *Synechococcus* sp. PCC 6312. Ca accumulation seems therefore to be more essential for *Cyanothece* sp. PCC 7425 and *G. lithophora* C7 than for *Synechococcus* sp. PCC 6312. Additional differences can be noted between *Synechococcus* sp. PCC 6312 and the two other ACC+ strains: while *Synechococcus sp.* PCC 6312 forms intracellular ACC granules in connection with cell division and between the cytoplasmic membrane and the outermost thylakoids, the two other strains form ACC granules in the center of the cells with no apparent connection with cell division (Benzerara et al., 2014; Blondeau et al., 2018a). Overall, intracellular carbonatogenesis likely follows different pathways in the clade of *Synechococcus* sp. PCC 6312 compared to other cyanobacteria and may have different functions. Li et al. (2016) suggested that in the clade of *Synechococcus* sp. PCC 6312, ACC may form by nucleating on cell division proteins such as FtsZ, which require relatively high Ca^{2+} for polymerization (e.g., Yu & Margolin 1997). If true, this needed amount of Ca may still remain relatively modest compared with the one required by other ACC+ cyanobacteria. Thereafter, we tentatively discussed potential causes for a higher demand in Ca observed for

524 *Cyanothece* sp. PCC 7425 and *G. lithophora* C7. Calcium may either be directly needed for
525 some biochemical processes and/or it may have a more indirect role through its involvement in
526 the formation of intracellular ACC which themselves fill a biological function. Calcium is
527 notoriously essential for bacteria (e.g., Dominguez, 2004). In particular, Ca is a co-factor for
528 cyanobacteria in the water-splitting in photosystem II complex (Debus, 1992). However, since
529 this need is shared by all cyanobacteria, it does not explain the observed higher requirement of
530 some of the ACC+ strains . Few studies have shown a similar need by other bacteria for
531 relatively high Ca concentrations. For example, Webb (1988) reported that the filamentous
532 bacterium, *Haliscomenobacter hydrossis*, grew better at Ca concentrations ≥ 0.69 mM and
533 suggested that relatively high concentrations of Ca may have been needed for the formation of
534 sheath by these bacteria. Shuttleworth and Unz (1991) showed that four strains of the
535 gammaproteobacterium *Thiothrix* sp. and one strain of the betaproteobacterium *Zoogloea*
536 *ramigera* need relatively high Ca concentrations for the formation of their sheath and mitigation
537 of the toxicity of heavy metals present in the culture media. However, since heavy metals were
538 only at trace concentrations in BG-11 and *Cyanothece* sp. PCC 7425, and *G. lithophora* C7 are
539 not filamentous, none of these functions apply to explain the differences in Ca requirements
540 between cyanobacterial strains forming intracellular ACC.

541 Similarly, high amounts of Ca are needed by sporulating bacteria (Stewart 1980)for
542 resistance of spores to wet heat (e.g., Kochan et al., 2018). Again, there is no obvious
543 connection with the cyanobacteria studied here, since they do not sporulate. Last, calcicytes in
544 the filamentous cyanobacterium *Mastigocoleus testarum* also accumulate large amounts of Ca
545 but this accumulation in a few cells has been proposed as a way to keep Ca concentration low
546 in the other cells, which does not apply to unicellular cyanobacteria such as the ones considered
547 here. Moreover, it has been suggested that the significant alkalization of the cytoplasm involved
548 by the presence of Ca^{2+} might be detrimental to the photosynthetic capacity of these cells.

549 Overall, unless a presently unknown biochemical process requiring high amounts of Ca
550 exists in cyanobacteria forming intracellular ACC only, it is possible that ACC+ strains require
551 high amounts of Ca so that they can form significant amounts of intracellular ACC, which are
552 beneficial to their growth. Several biological functions have been suggested for these ACC
553 granules in cyanobacteria by Couradeau et al. (2012) or for intracellular calcite in *A. oxaliferum*
554 (Gray & Head, 2014): 1) they may serve as ballasts for the cells as an adaptation to a benthic
555 form of life. However, this sounds unlikely since *Cyanothece* sp. PCC 7425, and *G. lithophora*
556 C7 were grown in the present study as planktonic cells. 2) Intracellular Ca-carbonates may
557 buffer intracellular pH and balance the formation of hydroxide by conversion of HCO_3^- to CO_2
558 upon carbon fixation. 3) Alternatively, they may serve as a storage form of inorganic carbon
559 available to the cells upon C-limited periods. Only future genetics studies providing mutants
560 impeded in their capability to form Ca-carbonates may help answering this question. Culturing
561 under C-limited conditions coupled with measurements of calcium carbonate dissolution may
562 be helpful too.

563 Whatever their cause, the observed differences in Ca requirement for growth between
564 cyanobacterial strains call for special care when attempting to culture and/or enrich these strains
565 from the environment. The BG-11 medium has proved to be a particularly useful generic growth
566 medium to culture a broad diversity of cyanobacterial strains (Rippka, Deruelles, Waterbury,
567 Herdman, & Stanier, 1979). Here, it is confirmed that 250 µM as a standard Ca concentration
568 provides a good compromise, allowing significant growth of strains forming intracellular
569 $CaCO_3$ and not being detrimental to strains not forming intracellular $CaCO_3$. However, for
570 enrichment cultures, which are performed over extended durations, strains not limited by Ca^{2+}
571 may be favored over time if Ca^{2+} has been consumed by those forming intracellular $CaCO_3$.
572 The use of BG-11 alone may therefore hinder the enrichment of the latter. Interestingly, it can
573 be noted that *G. lithophora* was successfully enriched by adding fragments of rocks containing

574 Ca-carbonates, which likely buffered the dissolved [Ca^{2+}] by constant Ca^{2+} input over
575 prolonged periods (Couradeau et al., 2012). Therefore, this strategy should be useful for future
576 studies aiming at enriching ACC+ cyanobacteria.
577
578
579 **Acknowledgments**
580 Funding for this work was provided by the European Research Council under European
581 Community's Seventh Framework Programme FP7/2007-2013 Grant 307110, ERC
582 CALCYAN. ADW was funded by French state funds managed by the ANR within the
583 Investissements d'Avenir programme under reference ANR-11-IDEX-0004-02, within the
584 framework of the Cluster of Excellence MATISSE. The Pasteur Culture Collection of
585 cyanobacteria was supported by the Institut Pasteur (M.G. and T.L.). The SEM facility at
586 IMPMC was purchased owing to funding by Région Ile de France Grant SESAME 2006 I-07-
587 593/R; the transmission electron microscopy facility at IMPMC was purchased owing to
588 funding by Region Ile de France Grant SESAME 2000 E 1435.

589 **References**

590 Altermann, W., Kazmierczak, J., Oren, A., & Wright, D. T. (2006). Cyanobacterial calcification
591 and its rock-building potential during 3.5 billion years of Earth history. *Geobiology*, *4*,
592 147-166.
593 Badger, M., & Andrews, T. (1982). Photosynthesis and inorganic carbon usage by the marine
594 cyanobacterium, *Synechococcus* sp. *Plant Physiology*, *70*, 517-523.
595 Barrán-Berdón, A., Rodea-Palomares, I., Leganes, F., & Fernandez-Pinas, F. (2011). Free Ca^{2+}
596 as an early intracellular biomarker of exposure of cyanobacteria to environmental
597 pollution. *Analytical and Bioanalytical Chemistry*, *400*, 1015-1029.
598 Belkin, S., & Boussiba, S. (1991). High internal pH conveys ammonia resistance in spirulina
599 platensis. *Bioresource Technology*, *38*, 167-169.
600 Benzerara, K., Skouri-Panet, F., Li, J., Ferard, C., Gugger, M., Laurent, T., … Moreira, D.
601 (2014). Intracellular Ca-carbonate biomineralization is widespread in cyanobacteria.
602 *Proceedings of the National Academy of Sciences of the United States of America*, *111*,
603 10933-10938.

Berkelman, T., Garret-Engele, P., & Hoffman, N. E. (1994). The pacL gene of Synechococcus sp. strain PCC 7942 encodes a Ca^{2+}-transporting ATPase. *Journal of Bacteriology*, *176*, 4430-4436.

BioMagnetech Corporation, (1990). Physical characteristics of magnetic bacteria and their electromagnetic properties in the frequency range of 1–400 GHz, *BioMagnetech Corporation*, New York.

Blondeau, M., Sachse, M., Boulogne, C., Gillet, C., Guigner, J.M., Skouri-Panet, F., … Benzerara, K. (2018a) Amorphous calcium carbonate granules form within an intracellular compartment in calcifying cyanobacteria. *Frontiers in Microbiology*, *9*, 1768.

Blondeau, M., Benzerara, K., Ferard, C., Guigner, J.M., Poinsot, M., Coutaud, M., … Skouri-Panet, F. (2018b). Impact of the cyanobacterium *Gloeomargarita lithophora* on the geochemical cycles of Sr and Ba. *Chemical Geology*, *483*, 88-97.

Boros, E., Kolpakova, M. (2018). A review of the defining chemical properties of soda lakes and pans: An assessment on a large geographic scale of Eurasian inland saline surface waters. *PLoS One, 13*, e0202205.

Bundeleva, I. A., Shirokova, L. S., Pokrovsky, O. S., Bénézeth, P., Ménez, B., Gérard, E., & Balor, S. (2014). Experimental modeling of calcium carbonate precipitation by cyanobacterium *Gloeocapsa* sp. *Chemical Geology*, *374-375*, 44-60.

Cam, N., Georgelin, T., Jaber, M., Lambert, J.-F., & Benzerara, K. (2015). In vitro synthesis of amorphous Mg-, Ca-, Sr- and Ba-carbonates: What do we learn about intracellular calcification by cyanobacteria? *Geochimica Et Cosmochimica Acta*, *161*, 36-49.

Cam, N., Benzerara, K., Georgelin, T., Jaber, M., Lambert, J.-F., Poinsot, M., … Cordier, L. (2016). Selective uptake of alkaline earth metals by cyanobacteria forming intracellular carbonates. *Environmental Science & Technology*, *50*, 11654–11662.

Cam, N., Benzerara, K., Georgelin, T., Jaber, M., Lambert, J.-F., Poinsot, M., … Jézéquel, D. (2018). Cyanobacterial formation of intracellular Ca-carbonates in undersaturated solutions. *Geobiology*, *16*, 49-61.

Chang, Y., Bruni, R., Kloss, B., Assur, Z., Kloppmann, E., Rost, B., … Liu, Q. (2014). Structural basis for a pH-sensitive calcium leak across membranes. *Science*, *344*, 1131-1135.

Clapham, D.E. (2007) Calcium signaling. *Cell, 131*, 1047-1058

Couradeau, E., Benzerara, K., Gerard, E., Moreira, D., Bernard, S., Brown, G. E., & Lopez-Garcia, P. (2012). An early-branching microbialite cyanobacterium forms intracellular carbonates. *Science*, *336*, 459-462.

Debus, R. J. (1992). The manganese and calcium ions of photosynthetic oxygen evolution. *Biochimica et Biophysica Acta (BBA) - Bioenergetics*, *1102*, 269-352.

Demaegd, D., Colinet, A.-S., Deschamps, A., & Morsomme, P. (2014). Molecular evolution of a novel family of putative calcium transporters. *PLoS ONE*, *9*, e100851.

Demain, A.L. & Solomon, N.A., (1981). Manual of industrial microbiology and biotechnology, *American Society for Microbiology*, Washington, DC.

Domínguez, D. C. (2004). Calcium signaling in bacteria. *Molecular Microbiology*, *54*, 291-297.

Domínguez, D. C., Guragain, M., & Patrauchan, M. (2015). Calcium binding proteins and calcium signaling in prokaryotes. *Cell Calcium*, *57*, 151-165.

Garcia-Pichel, F., Ramírez-Reinat, E., & Gao, Q. (2010). Microbial excavation of solid carbonates powered by P-type ATPase-mediated transcellular Ca^{2+} transport. *Proceedings of the National Academy of Sciences*, *107*, 21749-21754.

Gilabert, J. A. (2012). Cytoplasmic calcium buffering. In M. S. Islam (Ed.), Calcium signaling (pp. 483–498). Dordrecht: Springer Science & Business Media.

Golubic, S., & Lee S.-J., (1999). Early cyanobacterial fossil record: Preservation, palaeoenvironments and identification. *European Journal of Phycology*, *34*, 339-348.

Gonzalez-Esquer, C. R., Smarda, J., Rippka, R., Axen, S. D., Guglielmi, G., Gugger, M., & Kerfeld, C. A. (2016). Cyanobacterial ultrastructure in light of genomic sequence data. *Photosynthesis Research*, *129*, 147-157.

Gray, N. D. (2006). The unique role of intracellular calcification in the Genus *Achromatium*. In *Inclusions in Prokaryotes* (p. 299-309). Springer, Berlin, Heidelberg.

Gray, N., & Head, I. (2014). The Family Achromatiaceae. In E. Rosenberg, E. F. De Long, S. Lory, E. Stackebrandt, & F. Thompson (Éd.), *The Prokaryotes: Gammaproteobacteria* (p. 1-14). Berlin, Heidelberg: Springer Berlin Heidelberg.

Guida, B. S., & Garcia-Pichel, F. (2016). Extreme cellular adaptations and cell differentiation required by a cyanobacterium for carbonate excavation. *Proceedings of the National Academy of Sciences*, *113*, 5712-5717.

Guindon, S., Dufayard, J.-F., Lefort, V., Anisimova, M., Hordijk, W., & Gascuel, O. (2010). New algorithms and methods to estimate maximum-likelihood phylogenies: Assessing the performance of PhyML 3.0. *Systematic Biology, 59*, 307‑321.

Jansson, C., & Northen, T. (2010). Calcifying cyanobacteria—the potential of biomineralization for carbon capture and storage. *Current Opinion in Biotechnology*, *21*, 365-371.

Jiang, H.-B., Cheng, H.-M., Gao, K.-S., & Qiu, B.-S. (2013). Inactivation of Ca^{2+}/H^{+} exchanger in *Synechocystis* sp. strain PCC 6803 promotes cyanobacterial calcification by upregulating CO_2-concentrating mechanisms. *Applied and Environmental Microbiology*, *79*, 4048-4055.

Jones, G. E., Royle, L. G., & Murray, L. (1979). Cationic composition of 22 species of bacteria grown in seawater medium. *Applied and Environmental Microbiology*, *38*, 800-805.

Kamennaya, N. A., Ajo-Franklin, C. M., Northen, T., & Jansson, C. (2012). Cyanobacteria as biocatalysts for carbonate mineralization. *Minerals*, *2*, 338-364.

Kochan, T. J., Foley, M. H., Shoshiev, M. S., Somers, M. J., Carlson, P. E., & Hanna, P. C. (2018). Updates to *Clostridium difficile* Spore Germination. *Journal of Bacteriology*, *200*, e00218-18.

Krivtsov, V., Bellinger, E. G., & Sigee, D. C. (2005). Elemental composition of *Microcystis aeruginosa* under conditions of lake nutrient depletion. *Aquatic Ecology*, *39*, 123-134.

Lawford, H.G., & Rousseau, J.D., (1995). Establish medium requirements for high yield ethanol production from xylose by existing xylose-fermenting microorganisms. Technical Report NREL AAP-4-11195-03.

Lee, B. D., Apel, W. A., & Walton, M. R. (2004). Screening of cyanobacterial species for calcification. *Biotechnology Progress*, *20*, 1345-1351.

Li, J., Margaret Oliver, I., Cam, N., Boudier, T., Blondeau, M., Leroy, E., … Benzerara, K. (2016). Biomineralization patterns of intracellular carbonatogenesis in cyanobacteria: Molecular hypotheses. *Minerals*, *6*, 10.

Mansor, M., Hamilton, T. L., Fantle, M. S., & Macalady, J. (2015). Metabolic diversity and ecological niches of *Achromatium* populations revealed with single-cell genomic sequencing. *Frontiers in Microbiology*, *6*, 822.

Marchler-Bauer, A., Bo, Y., Han, L., He, J., Lanczycki, C. J., Lu, S., ... & Gwadz, M. (2016). CDD/SPARCLE: functional classification of proteins via subfamily domain architectures. Nucleic acids research, 45, D200-D203.

Merz, M. U. E. (1992). The biology of carbonate precipitation by cyanobacteria. *Facies*, *26*, 81-101.

Moreira, D., Tavera, R., Benzerara, K., Skouri-Panet, F., Couradeau, E., Gérard, E., … López-García, P. (2017). Description of *Gloeomargarita lithophora* gen. nov., sp. nov., a thylakoid-bearing, basal-branching cyanobacterium with intracellular carbonates, and proposal for Gloeomargaritales ord. nov. *International Journal of Systematic and Evolutionary Microbiology*, *67*, 653-658.

Nazarenko, L. V., Andreev, I. M., Lyukevich, A. A., Pisareva, T. V., & Los, D. A. (2003). Calcium release from *Synechocystis* cells induced by depolarization of the plasma membrane: MscL as an outward Ca^{2+} channel. *Microbiology*, *149*, 1147-1153.

Norland, S., Heldal, M., & Tumyr, O. (1987). On the relation between dry matter and volume of bacteria. *Microbial Ecology*, *13*, 95-101.

Novoselov, A. A., Silva, D., Schneider, J., Abrevaya, X. C., Chaffin, M. S., Serrano, P., … Filho, C. R. de S. (2017). Geochemical constraints on the Hadean environment from mineral fingerprints of prokaryotes. *Scientific Reports*, *7*, 4008.

Pokrovsky, O. S., Martinez, R. E., Golubev, S. V., Kompantseva, E. I., & Shirokova, L. S. (2008). Adsorption of metals and protons on *Gloeocapsa* sp. cyanobacteria: A surface speciation approach. *Applied Geochemistry*, *23*, 2574-2588.

Ponce-Toledo, R. I., Deschamps, P., López-García, P., Zivanovic, Y., Benzerara, K., Moreira, D. (2017) An early-branching freshwater cyanobacterium at the origin of chloroplasts. *Current Biology*, *27*, 1-6.

Price, G. D., Maeda, S., Omata, T., & Badger, M. R. (2002). Modes of active inorganic carbon uptake in the cyanobacterium, *Synechococcus* sp. PCC 7942. *Functional Plant Biology*, *29*, 131-149.

Ragon, M., Benzerara, K., Moreira, D., Tavera, R., & Lopez-Garcia, P. (2014). 16S rDNA-based analysis reveals cosmopolitan occurrence but limited diversity of two cyanobacterial lineages with contrasted patterns of intracellular carbonate mineralization. *Frontiers in Microbiology*, *5*, 331.

Riding, R. (2006). Cyanobacterial calcification, carbon dioxide concentrating mechanisms, and Proterozoic-Cambrian changes in atmospheric composition. *Geobiology*, *4*, 299-316.

Rippka, R., Deruelles, J., Waterbury, J., Herdman, M., & Stanier, R. (1979). Generic assignments, strain histories and properties of pure cultures of cyanobacteria. *Journal of General Microbiology*, *111*, 1-61.

Rouf, M. A. (1964). Spectrochemical Analysis of inorganic elements in bacteria. *Journal of Bacteriology*, *88*, 1545-1549.

Saghaï, A., Zivanovic, Y., Zeyen, N., Moreira, D., Benzerara, K., Deschamps, P., … López-García, P. (2015). Metagenome-based diversity analyses suggest a significant contribution of non-cyanobacterial lineages to carbonate precipitation in modern microbialites. *Frontiers in Microbiology*, *6*.

Saier, M. H., Reddy, V. S., Tsu, B. V., Ahmed, M. S., Li, C., & Moreno-Hagelsieb, G. (2016). The transporter classification database (TCDB): Recent advances. Nucleic Acids Research, *44*, 372-379.

Shuttleworth, K. L., & Unz, R. F. (1991). Influence of metals and metal speciation on the growth of filamentous bacteria. *Water Research*, *25*, 1177-1186.

Singh, S., & Mishra, A. K. (2014). Regulation of calcium ion and its effect on growth and developmental behavior in wild type and ntcA mutant of *Anabaena* sp. PCC 7120 under varied levels of $CaCl_2$. *Microbiology*, *83*, 235-246.

Stewart, M., Somlyo, A. P., Somlyo, A. V., Shuman, H., Lindsay, J. A., & Murrell, W. G. (1980). Distribution of calcium and other elements in cryosectioned *Bacillus cereus* T spores, determined by high-resolution scanning electron probe x-ray microanalysis. *Journal of Bacteriology*, *143*, 481-491.

Team R. C. (2013) R: A language and environment for statistical computing.

Thompson, J. D., Higgins, D. G., & Gibson, T. J. (1994). CLUSTAL W: improving the sensitivity of progressive multiple sequence alignment through sequence weighting, position-specific gap penalties and weight matrix choice. *Nucleic Acids Res*., *22*, 4673–4680.

van Veen, H. W., Abee, T., Kortstee, G. J. J., Konings, W. N., & Zehnder, A. J. B. (1994). Translocation of metal phosphate via the phosphate inorganic transport system of *Escherichia coli*. *Biochemistry*, *33*, 1766-1770.

Waditee, R., Hibino, T., Tanaka, Y., Nakamura, T., Incharoensakdi, A., & Takabe, T. (2001). Halotolerant cyanobacterium *Aphanothece halophytica* contains an Na^+/H^+ antiporter, homologous to eukaryotic ones, with novel ion specificity affected by C-terminal tail. *Journal of Biological Chemistry*, *276*, 36931-36938.

Waditee, R., Hossain, G. S., Tanaka, Y., Nakamura, T., Shikata, M., Takano, J., … Takabe, T. (2004). Isolation and functional characterization of Ca^{2+}/H^+ antiporters from cyanobacteria. *Journal of Biological Chemistry*, *279*, 4330-4338.

Webb, L. E. (1988). Calcium dependence of the filamentous bacterium *Haliscomenobacter hydrossis*. *Water Research*, *22*, 1317-1320.

Warren, L. A., & Ferris, F. G. (1998). Continuum between sorption and precipitation of Fe(III) on Microbial Surfaces. *Environmental Science & Technology*, *32*, 2331‑2337.

Yu, X. C., & Margolin, W. (1997). Ca^{2+}-mediated GTP-dependent dynamic assembly of bacterial cell division protein FtsZ into asters and polymer networks in vitro. *Embo Journal*, *16*, 5455-5463.

Supplementary information of "Evidence of high Ca uptake by cyanobacteria forming intracellular CaCO3 and impact on their growth"

Supplementary information file contains 1 table and 8 figures

Table S1. List of the studied cyanobacterial strains together with the main chemical data measured after their incubation in BG11.

Strains	Species	Final dissolved [Ca] (µM)	Uptake [Ca] (µM)	Dry weight (g/L)(± 1µg)	Final pH (± 0.01)	Incubation time (days)	Presence of intracellular ACC (yes/no)
C7	*Gloeomargarita lithophora*	6.3 ± 0.1	274.3	0.35	9.50	60	Yes
PCC 6301	*Synechococcus elongatus*	231.1 ± 1.6	49.6	0.49	10.56	40	No
PCC 6304	*Oscillatoria* sp.	209.6 ± 1.6	71.0	0.08	9.73	40	No
PCC 6306	*Leptolyngbya* sp.	257.2 ± 2.0	23.4	0.44	10.35	40	No
PCC 6307	*Cyanobium gracile*	217.5 ± 3.7	63.2	0.20	9.83	40	No
PCC 6308	*Geminocystis herdmanii*	229.0 ± 1.6	51.7	0.50	11.07	40	No
PCC 6312	*Synechococcus* sp.	29.9 ± 0.1	250.8	0.35	9.92	60	Yes
PCC 6506	*Kamptonema* sp.	257.3 ± 2.0	23.3	0.63	10.57	40	No
PCC 6603	*Synechococcus* sp.	12.7 ± 0.1	268.0	0.26	10.52	61	Yes
PCC 6605	*Chamaesiphon minutus*	207.3 ± 2.0	73.4	0.54	9.40	40	No
PCC 6712	*Chroococcidiopsis* sp.	210.9 ± 1.9	69.8	0.70	10.03	40	No
PCC 6715	*Synechococcus lividus*	7.4 ± 0.1	273.2	0.43	9.00	61	Yes
PCC 6716	*Synechococcus lividus*	40.6 ± 0.1	240.0	0.64	9.22	61	Yes
PCC 6717	*Synechococcus lividus*	77.1 ± 0.1	203.6	0.24	8.90	61	Yes
PCC 6802	*Pseudanabaena* sp.	237.6 ± 1.1	43.1	0.50	7.96	40	No
PCC 6803	*Synechocystis* sp.	203.0 ± 1.8	77.7	0.52	10.05	60	No
PCC 6903	*Pseudanabaena* sp.	240.4 ± 1.4	40.2	0.33	10.47	54	No
PCC 7103	*Calothrix* sp.	219.9 ± 3.3	60.8	0.88	10.42	47	No
PCC 7104	*Leptolyngbya* sp.	232.1 ± 3.4	48.6	1.03	10.70	40	No
PCC 7107	*Nostoc* sp.	240.0 ± 3.6	40.6	0.42	10.17	47	No
PCC 7113	*Microcoleus* sp.	267.2 ± 3.2	13.5	0.68	9.36	47	No
PCC 7120	*Nostoc* sp.	240.4 ± 2.9	40.3	0.41	9.71	47	No
PCC 7122	*Anabaena aequalis*	250.7 ± 2.6	29.9	0.40	9.14	54	No
PCC 7203	*Chroococcidiopsis thermalis*	112.5 ± 0.7	168.2	1.03	9.99	61	Yes
PCC 7327	*Pleurocapsa sp.*	249.5 ± 1.9	31.2	0.39	9.21	54	No
PCC 7407	*Geitlerinema sp.*	245.3 ± 1.7	35.3	0.09	8.95	54	No

PCC 7408	*Pseudanabaena catenata*	297.8 ± 0.7	0.0	1.19	10.04	54	No
PCC 7417	*Cylindrospermum stagnale*	250.5 ± 1.0	30.1	1.26	9.71	40	No
PCC 7424	*Cyanothece* sp.	214.6 ± 1.3	66.0	0.56	9.77	54	No
PCC 7425	*Cyanothece* sp.	28.1 ± 0.1	252.6	0.57	9.37	60	Yes
PCC 7428	*Gloeocapsa* sp.	173.4 ± 0.8	107.2	0.52	9.48	54	No
PCC 7429	*Pseudanabaena* sp.	241.4 ± 1.7	39.2	0.30	10.07	54	No
PCC 7432	*Chroococcidiopsis* sp.	42.6 ± 0.1	238.1	1.08	10.25	61	Yes
PCC 7433	*Chroococcidiopsis* sp.	59.3 ± 0.3	221.4	0.80	10.25	61	Yes
PCC 7434	*Chroococcidiopsis* sp.	50.4 ± 0.2	230.2	0.74	10.2	61	Yes
PCC 7437	*Stanieria cyanosphaera*	239.5 ± 1.3	41.2	0.82	9.51	54	No
PCC 7439	*Chroococcidiopsis* sp.	106.3 ± 0.8	174.3	0.63	9.95	61	Yes
PCC 7507	*Calothrix*	270.5 ± 5.0	10.1	1.17	9.99	54	No
PCC 7509	*Synechocystis* sp.	261.0 ± 1.4	19.6	0.36	9.92	54	No
PCC 7524	*Nostoc sp.*	227.0 ± 0.7	53.6	0.72	9.41	40	No
PCC 7942	*Synechococcus elongatus*	305.9 ± 1.0	0.0	0.67	9.83	40	No
PCC 8303	*Cyanothece* sp.	116.1 ± 0.8	164.5	0.39	10.7	61	Yes
PCC 8801	*Cyanothece* sp.	264.7 ± 0.9	15.9	0.40	9.79	47	No
PCC 8955	*Cyanothece* sp.	61.0 ± 0.2	219.7	0.39	8.73	61	Yes
PCC 9009	*Tolypothrix* sp.	253.9 ± 2.0	26.7	0.26	10.14	47	No
PCC 9308	*Cyanothece* sp.	12.6 ± 0.1	268.0	0.29	8.74	61	Yes
PCC 9431	*Fischerella* sp.	233.9 ± 0.6	46.8	1.19	9.01	47	No
PCC 9819	*Chroococcidiopsis* sp.	39.7 ± 0.1	240.9	1.16	9.35	61	Yes
PCC 10605	*Cyanobacterium aponinum*	252.5 ± 1.8	28.2	0.43	9.48	47	No
PCC 10802	*Oscillatoria princeps*	254.2 ± 2.2	26.5	4.24	10.08	47	No
PCC 73102	*Nostoc punctiforme*	263.4 ± 0.6	17.2	0.34	9.59	47	No
PCC 73106	*Gloeocapsa* sp.	256.7 ± 2.1	24.0	0.20	8.88	47	No

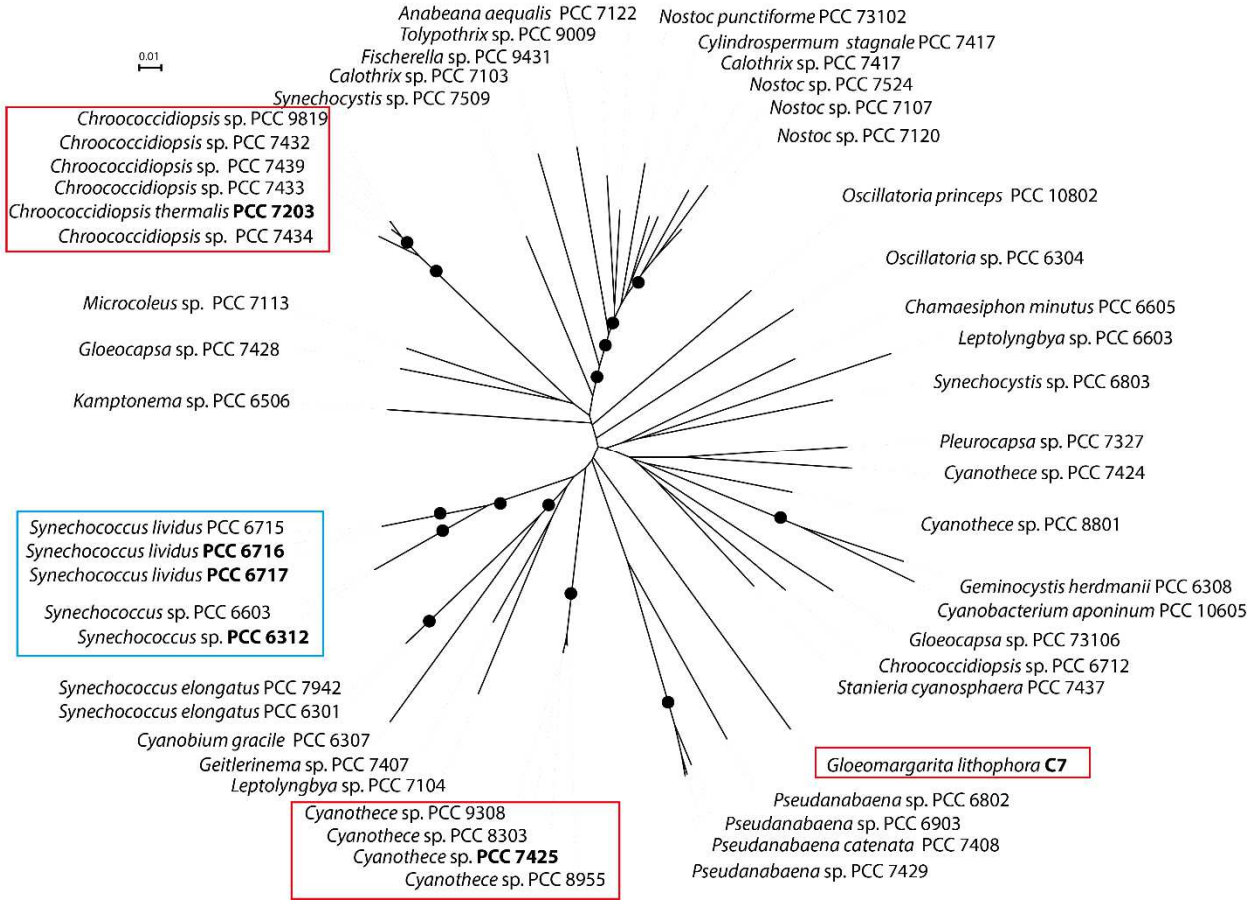

Figure S1. PhyML phylogenetic tree of the 52 tested strains based on the 16S rRNA gene. Nodes supported at 70% or more are indicated by a black dot. The ACC+ strains are outlined by a red square for granules scattered throughout the cells and a blue square for cells with granules located at cell poles and septa. The ACC+ strains described by Benzerara et al. (2014) are highlighted in bold.

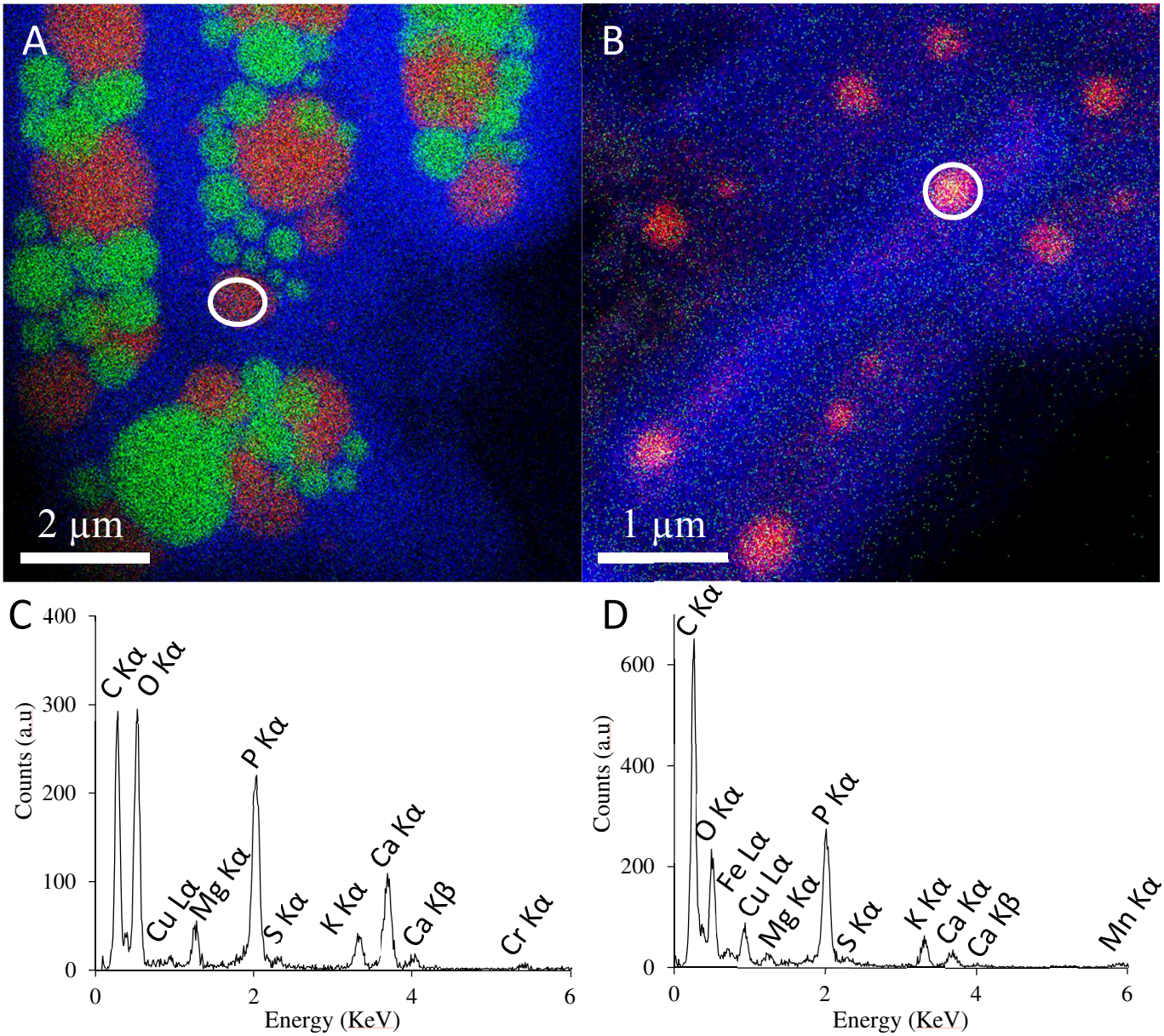

Figure S2. STEM-EDXS analyses of the ACC+ *Cyanothece* sp. PCC 9308 and the ACC- *Synechococcus elongatus* PCC 6301 strains grown in BG-11. (A) STEM-EDXS map of a cell of *Cyanothece* sp. PCC 9308. (B) STEM-EDXS map of a cell of *Synechococcus elongatus* PCC 6301. (C) EDXS spectrum of the PolyP inclusion of *Cyanothece* sp. PCC 9308 outlined by a white circle in (A). (D) EDXS spectrum of the PolyP inclusion of *Synechococcus elongatus* PCC 6301 outlined by a white circle in (B). For all EDXS maps, calcium is in green, phosphorus in red and carbon in blue. As a result, Ca-carbonates appear in green and PolyP granules in red.

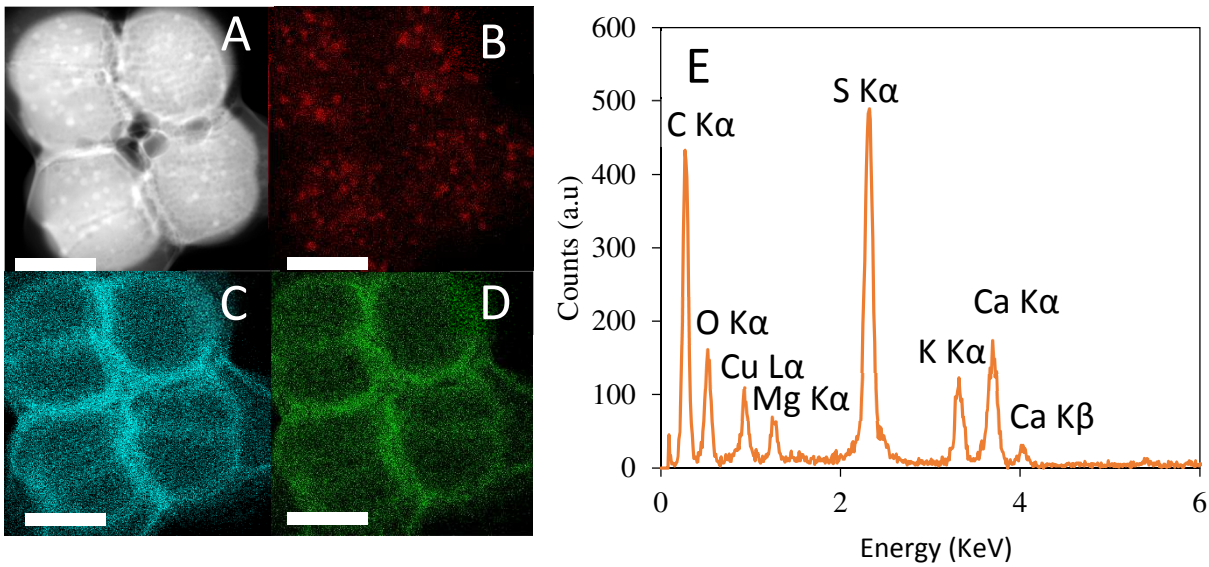

Figure S3. STEM analyses of *Gloeocapsa* sp. PCC 7428 cells grown in BG-11. (A) STEM-HAADF image. (B) STEM-EDXS maps of phosphorus. (C) STEM-EDXS map of sulfur. (D) STEM-EDXS map of calcium. (E) EDXS spectrum of the cell wall of the cells. The scale bar represents 2 µm.

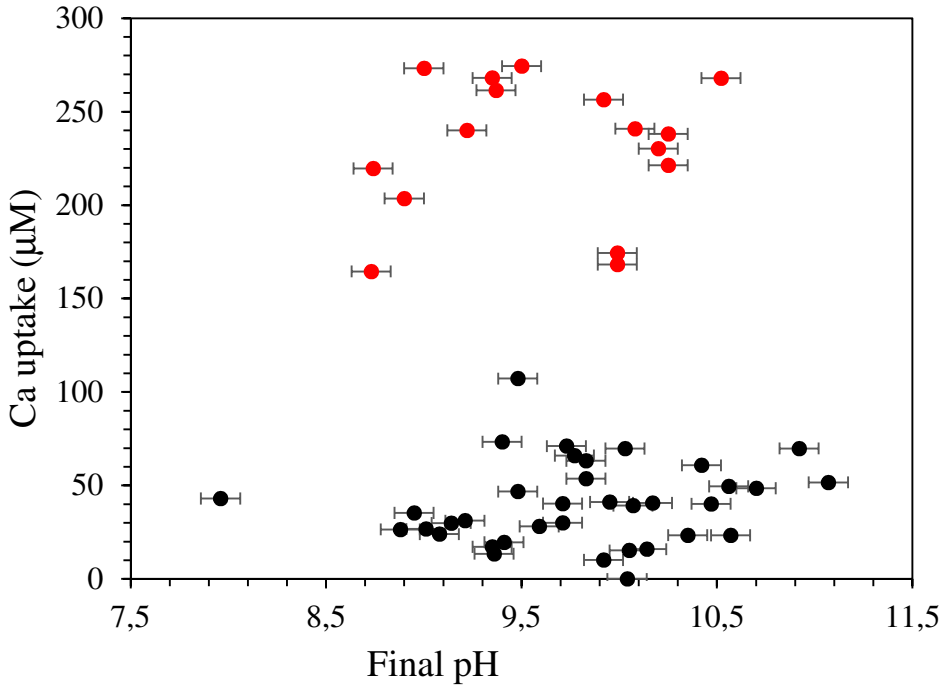

Figure S4. Calcium uptake (obtained by subtracting the dissolved Ca concentration left after cell incubation from the initial dissolved Ca concentration in the culture medium) *vs* pH for the 52 cyanobacterial strains. In red: strains producing intracellular ACC; in black: strains not forming intracellular ACC.

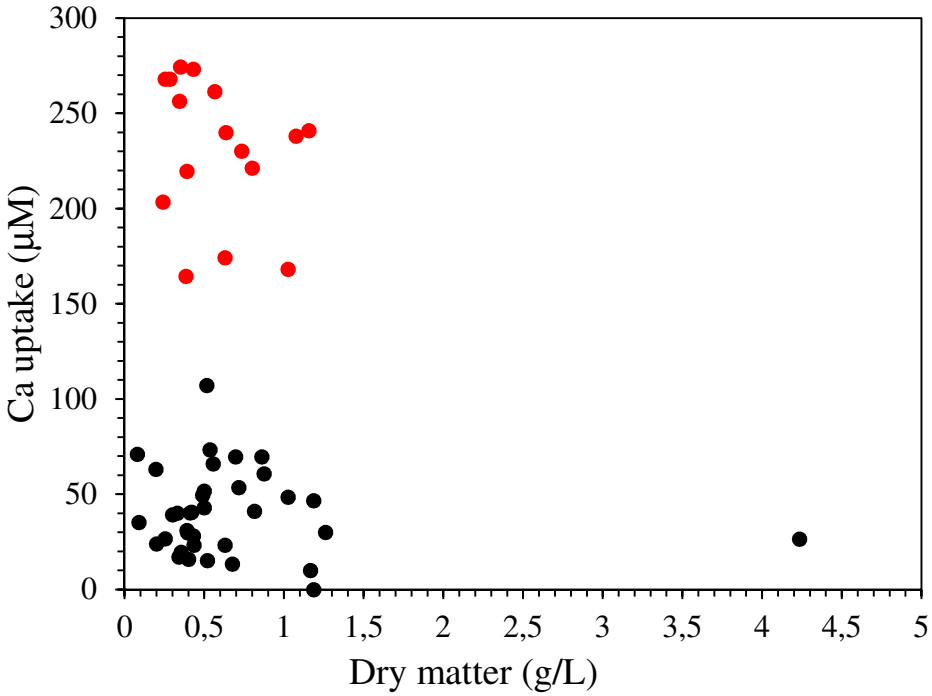

Figure S5. Calcium uptake (obtained by subtracting the dissolved Ca concentration left after cell incubation from the initial dissolved Ca concentration in the culture medium) vs dry mass for the 52 cyanobacterial strains of cyanobacterial. In red: strains producing intracellular ACC; in black: strains not forming intracellular ACC.

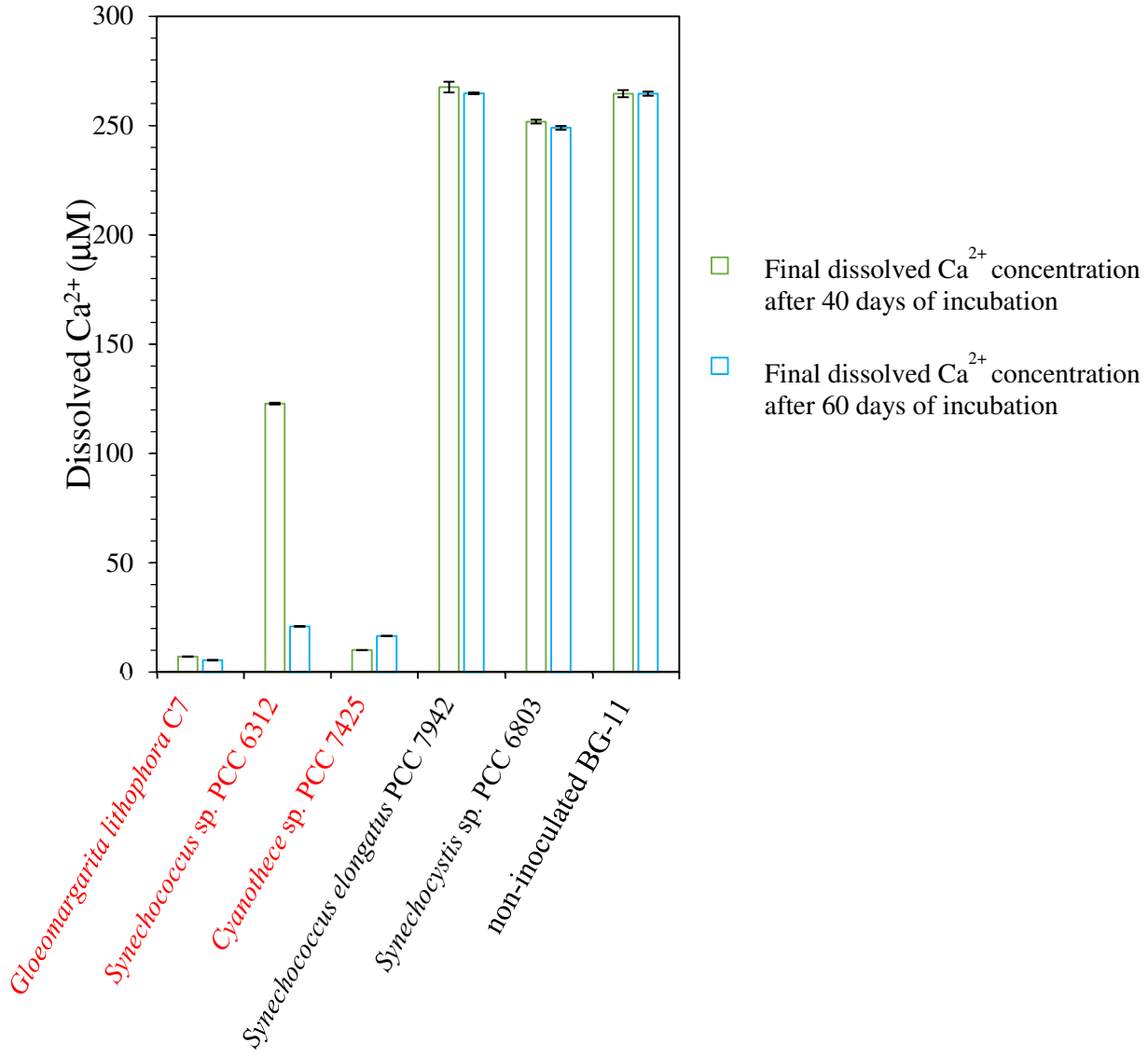

948

949 **Figure S6.** Final dissolved calcium concentration for cultures grown in sterile BG-11 after 40 (green)
950 and 60 (blue) days of incubation. Strains forming intracellular ACC (*G. lithophora*, *Synechococcus* sp.
951 PCC 6312, *Cyanothece* sp. PCC 7425) are indicated in red, and strains without ACC (*Synechococcus*
952 *elongatus* PCC 7942, *Synechocystis* sp. PCC 6803) are indicated in black. Error bars were calculated
953 based on the precision of ICP-AES measurements.

954

955

956

957

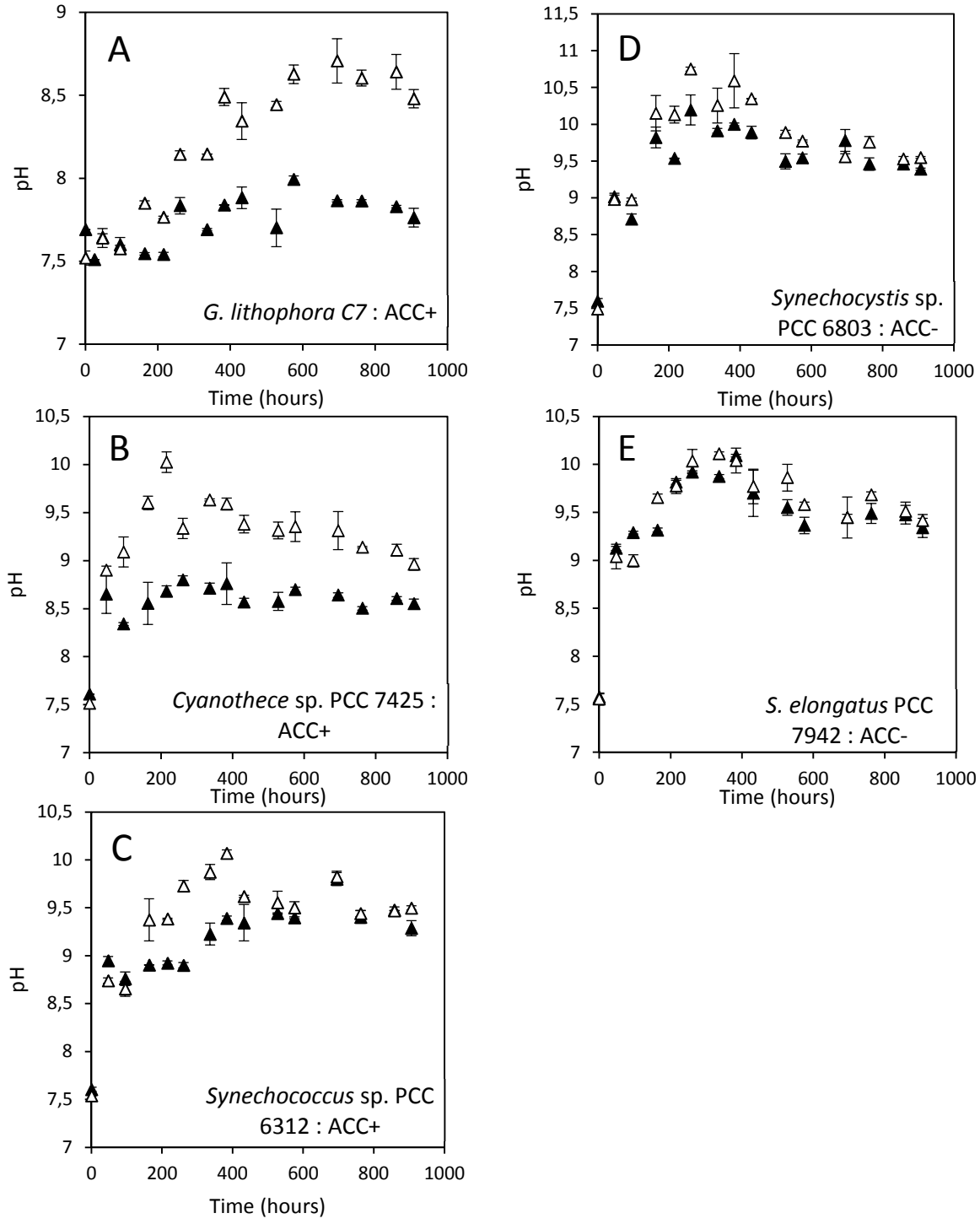

Figure S7. Time variations of pH in cultures with an initial Ca concentration of 50 µM (closed symbols) and 250 µM (open symbols). (A) *G. lithophora* C7; (B): *Cyanothece* sp. PCC 7425; (C): *Synechococcus* sp. PCC 6312; (D): *Synechocystis* sp. PCC 6803; (E): *Synechococcus elongatus* PCC 7942. Error bars represent standard deviations calculated based on variations between duplicates.

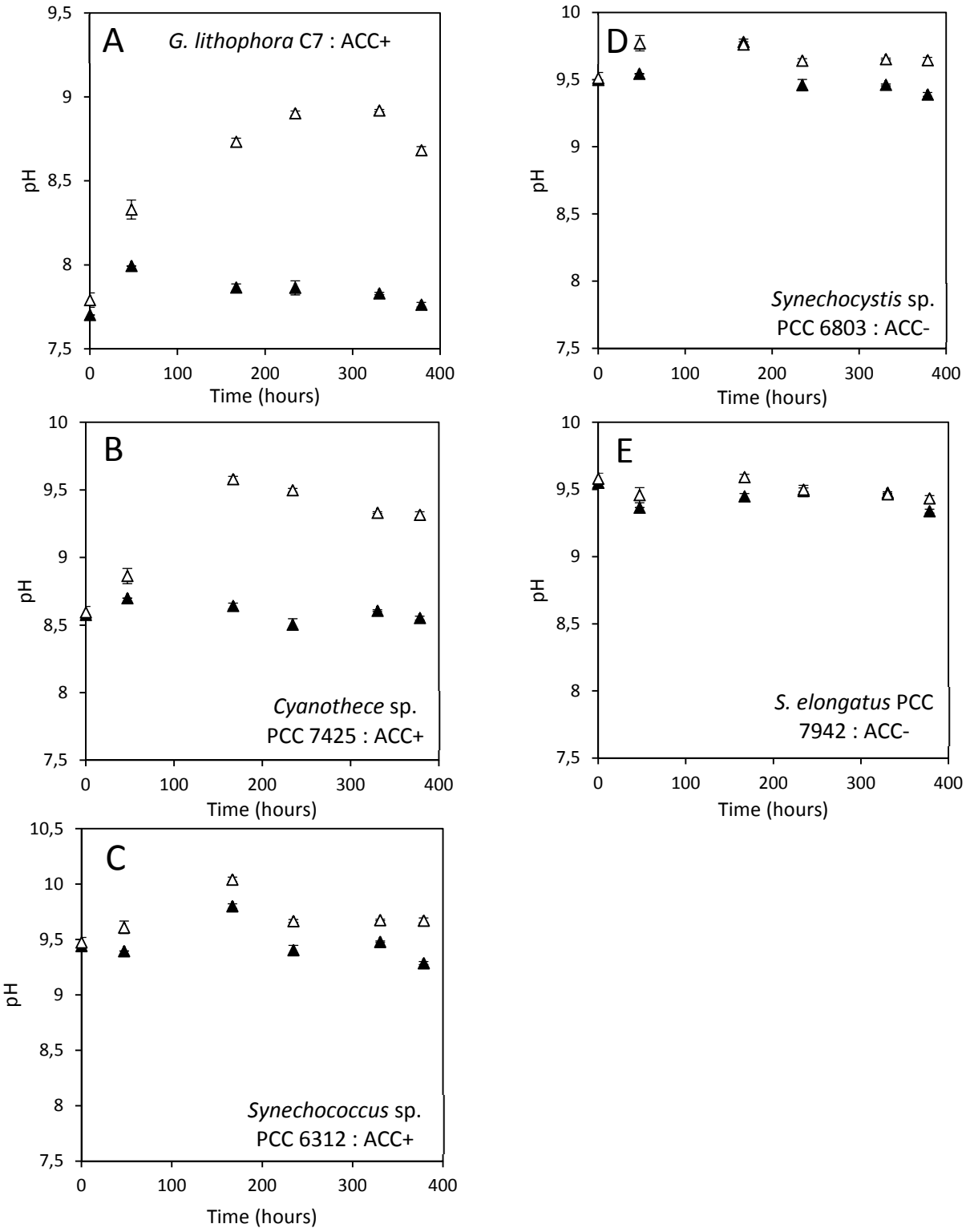

963
964 **Figure S8.** Time evolution of pH measured in subcultures first grown in BG-11 with 50 µM of Ca, then
965 supplemented (open symbols) or not (closed symbols) with 200 µM of Ca. Addition of 200 µM of Ca
966 was done at t=0. (A) *G. lithophora* C7; (B) *Cyanothece* sp. PCC 7425; (C) *Synechococcus* sp. PCC
967 6312; (D) *Synechocystis* sp. PCC 6803; (E) *Synechococcus elongatus* PCC 7942. Error bars represent
968 standard deviations calculated based on variations between duplicates.

969